7-1973

Electron-Beam Retardation Contact Potential of Cuprous Oxide

James Lindle
Western Kentucky University

Lindle,

James Ryan

1973

ELECTRON-BEAM RETARDATION CONTACT POTENTIAL OF CUPROUS OXIDE

A Thesis

Presented to

the Faculty of the Department of Physics and Astronomy

Western Kentucky University

Bowling Green, Kentucky

In Partial Fulfillment

of the Requirements for the Degree

Master of Science

by

James Ryan Lindle

July 1973

ELECTRON-BEAM RETARDATION CONTACT

POTENTIAL OF CUPROUS OXIDE

N. T. Tit
Director of Thesis

N. T. Tit

George P. Brown

D. L. Humphreys

Approved Aug. 2, 1973
Date

Elmer Grim
Dean of Graduate College

Approved August 13, 1973
Date

ACKNOWLEDGEMENT

I would like to acknowledge the assistance and guidance given me in the preparation of this thesis by Dr. Richard Komp. His guidance in a period that was very trying to him made this thesis possible.

I would also like to acknowledge the assistance of Dr. George Moore who helped me produce this manuscript. I appreciate the assistance given me by Bill Courtney and Alonso Alexander in the design and construction of my apparatus and in the production of the drawings found in this manuscript. Guy Briggs produced the excellent photographs and Gary Dillard produced the photomicrographs.

ABSTRACT

The purpose of this research is to determine the contact potential difference of cuprous oxide, Cu_2O, with respect to gold. A band model for cuprous oxide is presented.

Single-crystal cuprous oxide is prepared from Oxygen Free High Conductivity copper equilibrated at 1020°C and at atmospheric pressure. The contact potential difference of cuprous oxide (using gold as a reference) is measured in a bakeable ultrahigh vacuum system using a modified version of Nelson's electron beam retardation method. Measurements made at 10^{-6} torr and at room temperature give a value of 0.1 ±0.05 eV for the contact potential difference of cuprous oxide with respect to gold.

Photoelectric emission from the gold reference is approximately 4.9 eV. Hence, the Fermi level resides at approximately 5 eV below vacuum zero. This places the Fermi level between the valence band which was found to be at approximately 5.1 eV and the acceptor levels which reside somewhere between 0.3 eV and 0.6 eV above the valence band. From optical experiments the band width has been determined to be approximately 2.3 eV. If 5.1 eV is taken as the top of the valence band and 2.3 eV is the band gap, then the electron affinity of cuprous oxide is approximately 2.8 eV.

TABLE OF CONTENTS

LIST OF ILLUSTRATIONS

LIST OF TABLES

INTRODUCTION

Properties of Cuprous Oxide

Since the 1920's cuprous oxide, Cu_2O, has undergone extensive investigation. Early interest stemmed from the known rectifying and photovoltaic properties of cuprous oxide. Although the mechanisms of these phenomona were unknown, rectifiers and photovoltaic cells of cuprous oxide were used long before the present theory of semiconductor behavior was developed. In the 1930's, many studies were undertaken on the photoelectric properties of cuprous oxide. However, cuprous oxide presented many complexities absent in simplier systems; such as, silicon and germanium. In the early 1940's interest in cuprous oxide diminished. After World War II the interest in cuprous oxide was revitalized and investigations were begun on the optical and conductivity properties of the material. In recent years these interests have grown to include studies of band structure in cuprous oxide.

Much of the work on cuprous oxide, especially the early investigations must be viewed with skepticism. The use of polycrystalline materials (materials composed of several crystals separated by grain boundaries) cast forboding shadows on many of the earlier investigations. Today, the important role that grain boundaries and surfaces play in the properties of cuprous oxide is recognized [1]. Another

shortcoming arises from insufficient precautions to maintain the samples within the temperature - oxygen pressure stability zone for cuprous oxide. This will be discussed in more detail shortly. Many early researchers did not specify the exact sample environment; for example, the pressure under which measurements were taken or the oxygen pressures and temperatures used in growing the crystals.

The stability curve (Figure 1) of the copper - oxygen system shows the oxygen pressure versus temperature zone for which cuprous oxide is stable. It is intuitively obvious that work cannot always be done in the cuprous oxide stability region. However, if a transition to room temperature occurs quickly enough the high temperature composition is "frozen in", although oxygen diffusion will still produce surface imperfections. Even though cuprous oxide in air is not thermodynamically stable at room temperature, it reacts so slowly that cuprous oxide is kinetically stable in air and thus, short term aging effects can be neglected. At a temperature range from 100°C to 500°C, the reaction of cuprous oxide is too slow to reach equilibrium but too fast to be ignored. Consequently, this region must be avoided. Figure 1 also shows the equilibration points used in this work.

Cuprous oxide is a compound composed ideally of two copper atoms and a single oxygen atom. As early as 1930, the departure of cuprous oxide from the stoichioretric ratio of 2:1 in the direction of excess oxygen was known. The

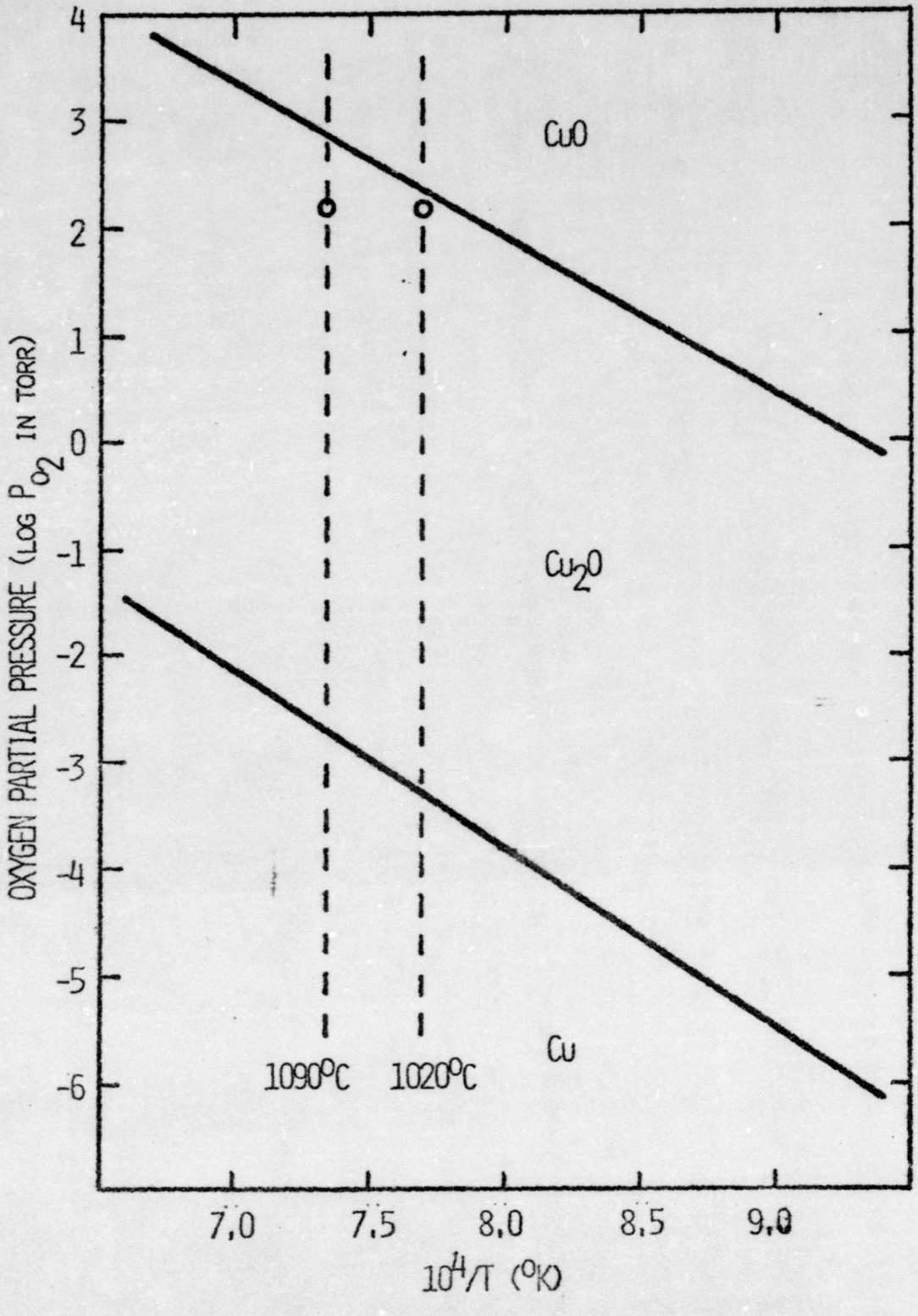

FIGURE 1. PHASE DIAGRAM FOR COPPER-OXYGEN SYSTEM.

excess oxygen in cuprous oxide crystals was noted to increase with an increase in oxygen partial pressure. The effect of increasing the excess oxygen on the electrical properties of cuprous oxide was predicted by Wagner[2] (1938) to increase the conductivity as the one-eigth the power of the oxygen pressure. More recently, studies by Hogarth[3] and M. H. Zirin and Trivich[4] on the thermoelectric properties of cuprous oxide have verified Wagner's work.

Electrical conductivity in cuprous oxide depends on the conduction of holes. Without exception, cuprous oxide is known as a P-type semiconductor. Wright[5] and Zirin and Trivich[4] failed to produce N-type cuprous oxide although Trivich suggests the possibility of N-type cuprous oxide at very low oxygen pressures.

Figure 2 depicts the band structure of a P-type semiconductor. The height of the Fermi level, E_F, above the valence band depends primarily upon the concentration and distribution of acceptor levels. The number of ionized acceptor states depends upon the temperature in accordance with the Fermi-Dirac distribution. At room temperature, the Fermi level resides somewhere between the valence band and the acceptor levels. The magnitude of the Fermi energy (that is the energy required to move an electron from the Fermi level to a rest position just exterior to the surface) is defined as the work function of the material.

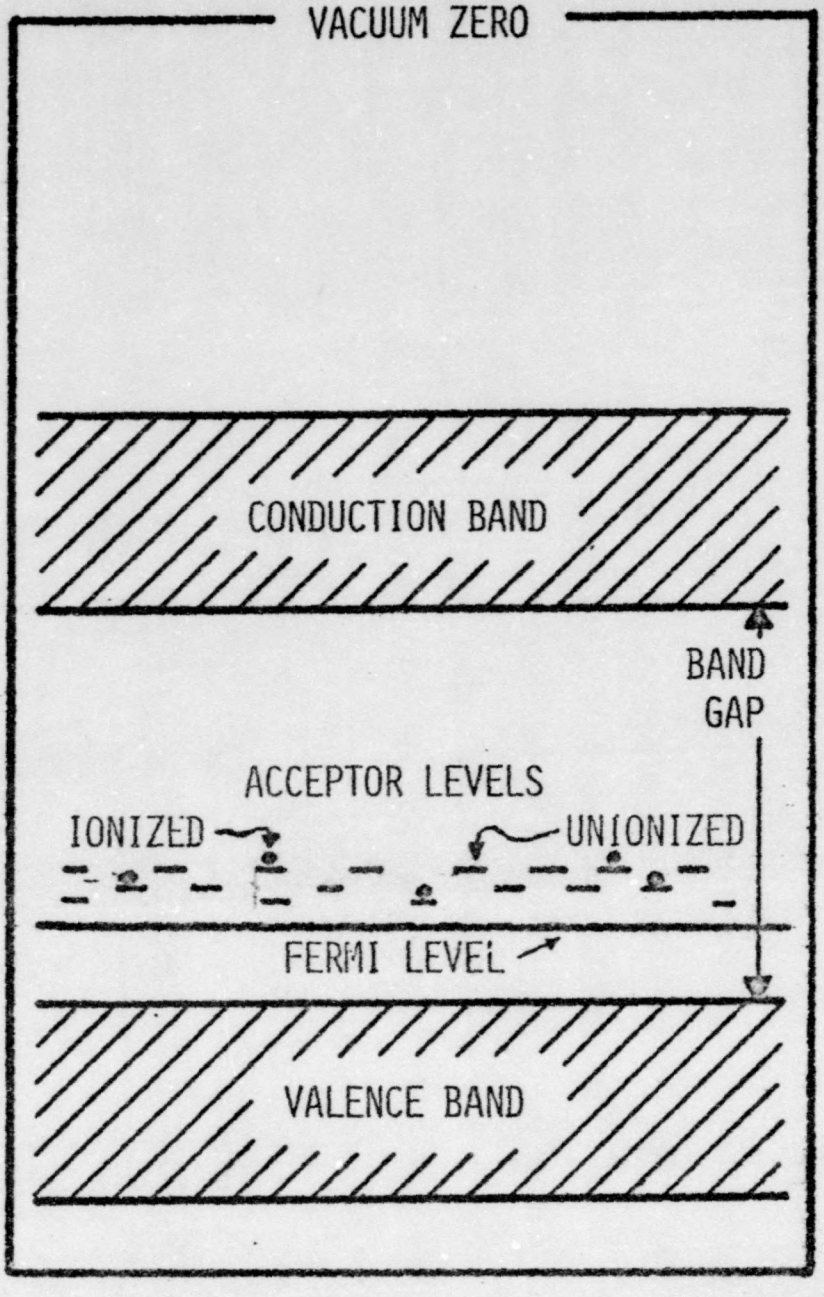

FIGURE 2. ENERGY BAND IN P-TYPE SEMICONDUCTORS.

The energy of acceptor levels in cuprous oxide has been investigated by several researchers. Fortin and Weichman[6], in extending the work of Wright[5], investicated the dependence of hole mobility upon temperature (25°C to 800°C) and, together with Hall-effect measurements, located acceptor levels at 0.3 eV to 0.6 eV, 1.0 eV, and 1.6 eV above the valence band. The 1.0 eV and 1.6 eV levels do not exist in the temperature range considered in this study. These levels are characteristic of samples heated above 125°C which causes a high-conductivity surface layer to redistribute itself throughout the bulk producing an oxygen rich layer beneath the surface. However, the 0.3 eV to 0.6 eV levels were found to be characteristic of fresh samples subjected to low temperatures. If a sample were exposed to air for some time, the electrical conductivity became a surface effect quite independent of the bulk properties. More recent studies by Kuzel and Weichman[7] are in agreement with the energy of the acceptor levels. In this research, the surface of cuprous oxide is studied rather than the bulk although at thermal equilibrium in the absence of band bending the properties should be identical.

The position of the top of the valence band with respect to the vacuum zero has been measured by Komp[8] using values obtained from the high-energy threshold of photoelectric emission. The high-energy threshold corresponds to the energy of direct transition with scattering of photoelectrons from the valence band. From these

measurements the top of the valence band was found to be 5.09 ±0.05 eV with respect to vacuum zero. An independence of this threshold upon surface band bending and upon the temperature and the oxygen pressure of sample preparation was observed.

Another measurement of the photoelectric emission from cuprous oxide was made by Ioffe[9] in the early 1950's. At that time, Ioffe's value of 5.15 eV was accepted as the work function of cuprous oxide. However, from the previous discussion, this value is known to be the high-energy threshold of photoemission which gives the energy of the top of the valence band rather than the work function. Note that this value is in good agreement with the value obtained by Kemp.

With this knowledge, the limits on the Fermi energy can be given numerically. Since the Fermi level must be above the valence band (otherwise, it would portray metallic properties), its magnitude must be less than the high-energy threshold, which is approximately 5.1 eV. Unless the acceptor levels are completely ionized (a condition incompatible with the observed temperature dependence of conductivity), the lower limit of the Fermi level for an extrinsic semiconductor is the magnitude of the acceptor levels which lie at 0.3 eV to 0.6 eV above the top of the valence band. Thus the Fermi level has the following limits

$$5.1 \text{ eV} \geq E \geq 4.5 \text{ eV}$$

Work Function

The magnitude of the Fermi energy (the minimum energy necessary to remove an electron from the Fermi level to vacuum zero) is defined as the work function, ϕ, of cuprous oxide. Physically stated, the work function is the magnitude of the work required to move an electron from the interior of a metal to a rest position just exterior to the surface. The magnitude of the work function is a few eV (approximately 5 eV for cuprous oxide) and can be expressed as

$$\phi = e\ CPD$$

where CPD is the contact potential difference with vacuum and e is the electronic charge.

If the work function of a substance such as gold can be consistently determined, then the contact potential between this standard and a sample (cuprous oxide) gives the difference in their work functions. Thus, the work function of the material is related to the known work function of the reference through the measurement of their contact potential difference:

$$\phi\ (sample) = \phi\ (reference) + CPD$$

It is not necessary that the reference and the sample be in physical contact though their separation should be minimized and their environment, an ultra high vacuum.

The difference in the work function of two substances is defined as their contact potential difference. Common

methods of measuring the contact potential difference are: the Kelvin method, the ionization method, and the Nelson electron-beam retardation method. Here, the ionization method is of little interest because in high vacuum no ionization between the sample and the alpha-emitter takes place. However, measurements made in ionized air are accurate to 0.01 V.

In contrast, the Kelvin method is used quite extensively in ultra high vacuum systems. If a vibrating capacitor is incorporated in the Kelvin method it is accurate to 0.01 V. This method is sensitive to surface contamination and disorders but insensitive to interactions between electrons and patch fields. This latter property is the criterion upon which Anderson[10] directly compared the Kelvin method with the electron-beam retardation method. Anderson found that the measurements made on silver and barium by both methods were in agreement to within experimental error limits. He noted that the electron beam method is sensitive to patch interactions, and therefore the electron beam method gives the average work function.

Nelson's electron beam retardation method was used in this study to determine the contact potential difference of cuprous oxide with a gold reference. An electron beam with an energy characteristic of the gun's work function is directed at a sample while the potential between the gun and the sample is varied. The sample electron beam current has a maximum when the potential of the gun filament is slightly

negative compared to the sample. This potential is the sum of both the contact potential difference between the gun and the sample and the external bias applied to the gun. If the experiment is repeated on a reference material, a curve of identical shape results and the horizontal displacement of these curves is the contact potential difference.

Originally, Nelson[11] developed the electron-beam retardation method to measure the electron affinity of organic semiconductors. Electrons in covalent-bonded materials are localized to a single molecule so that the number of free electrons present in the conduction band of organic semiconductors is very small. When an electron beam strikes an organic semiconductor, the electron distribution is altered drastically as the electrons enter the conduction band. Komp[12] notes that sulfur and selenium exhibited a space charge effect at beam currents higher than 10^{-13} A. Thus the retardation potential compared to a known reference gives the energy of the conduction band relative to vacuum zero; that is, the electron affinity.

In cuprous oxide the distribution of electrons is relatively unaffected by a beam current of 10^{-11} A. If electrons are projected at cuprous oxide, then the retardation potential compared to a known reference gives the energy of the Fermi level relative to vacuum zero; that is, the work function.

Direct determination of the work function of a metal is possible through emission experiments. Common methods of

producing emission from metals are by thermal or photo-excitation or by producing large electric fields in the vacuum just exterior to the sample. If the properties of the solid are invariant to the temperature necessary to produce a measurable saturation current (cuprous oxide is not such a material), the Richardson law yields the work function since the work function is the only term in the equation that is characteristic of the solid.

Field emission gives the work function of metals but does not give the true work function of semiconductors since high fields produce degenerate surface states. By producing a sufficiently large field just outside the metallic surface, electrons are given enough energy to escape the metal. The current is related to the work function according to the Fowler and Nordheim relationship. Recently, field electron microscopes incorporating the field emission theory have been used to measure the work function of metals.

Contamination and Surface Effects in Metals

Anderson[13] and Huber[14] have investigated the effects of contamination on the work function of metals. Anderson in measuring the work function of gold found "erratic and marked drifts in the contact potential occurred on aging for a period of one to two days." Also, in an article on the work function of copper, Anderson[15] notes a "rapid drift

towards lower work function on aging" and "poor reproducibility" due to absorbed gases. Huber[14] studied the effects of mercury contamination on the work function of gold, silver, and aluminium. Huber found that mercury contamination affected the three metals differently. Mercury was extremely reactive with gold and had a high "sticking coefficient" with the gold surface. Upon comparing the work function of mercury-contaminated gold with clean gold, Huber found a discrepancy of approximately 0.5 eV. Mercury apparently lowered the work function. Since most earlier studies were undertaken in mercury systems, his theory appears consistent because earlier values of the work function of gold were lower by about 0.5 eV.

Anderson[16] also investigated the effects of the double layer on the work function of lithium and sodium. Using the equation

$$\phi = \phi \text{ (volume)} + \phi \text{ (surface)}$$

obtained from the work of Wigner and Bordeen[17], Anderson determined the contribution of the surface double layer to be of the order of 0.3 eV. He concluded that the surface double layer is relatively unimportant in determining the work function of monovalent metals. The effect of the surface layer would be even less when using the electron-beam retardation method.

Photoelectric Emission from Metals

In the early 1930's, the basic theory of photoelectric emission from metals was developed by Fowler[18]. Since then this theory has been used extensively to find the work function of metals and the position of the valence band in extrinsic semiconductors. When light of sufficiently high energy strikes a solid, electron emission occurs. However, emission can occur with high probability only if hv (where h is Planck's constant and v is the frequency) is greater than or equal to the work function because the energy states above the Fermi level are sparsely occupied.

For metals, the photoelectric threshold is identical to the work function. The photoelectric threshold can be found by comparing two plots: hv/kT versus the $\log(Y/T^2)$ where, Y is the photoelectric yield, k is the Boltzmann's constant and T is the absolute temperature, and $\bar{\Phi}(u)$ versus u. These curves have the same shape. Here, according to Fowler's theory $\log (Y/T^2)$ is equal to B + $\bar{\Phi}(u)$ where $\bar{\Phi}(u)$ is a universal function of u ($u = [h(v - v_o)]/kT$) given by

$$\bar{\Phi}(u) = \log_{10} (e^{u} - e^{2u/4} + e^{3u/4} + ...) \text{ for } u \leq 0$$

$$\bar{\Phi}(u) = \log_{10} \left(\frac{\pi}{6} + \frac{u^2}{2} - [e^{-u} - \frac{e^{-2u}}{4} + \frac{e^{-3u}}{9} + ...] \right) \text{ for } u \geq 0$$

and B is a constant, independent of v or T. Where the experimental and theoretical curve coincide, the hv/kT value on the experimental curve corresponding to u = 0 ($h\nu = h\nu_o$) on the theoretical curve is read directly from the graph. The theoretical curve and values of $\bar{\phi}(u)$ versus u are shown in Figure 3.

Fowler[18], in his article developing the photoelectric theory, indicates another method to find ν_o. When $\bar{\phi}(u)$ is observed in a region approaching zero from the positive sense, then the yield is

$$Y = C(\nu - \nu_o)^2$$

where C is a constant. A plot of $Y^{1/2}$ versus ν is a straight line in the vicinity of the threshold and an extrapolation to Y = 0 can be used to calculate ν_o.

Photoemission and Semiconductors

As previously indicated, the photoelectric emission threshold for extrinsic semiconductors is not, in general, the work function. This is because the Fermi level in semiconductors is not usually at the same energy as available levels and, thus, no electrons in general exist at the Fermi level. Instead, many energy states exist from

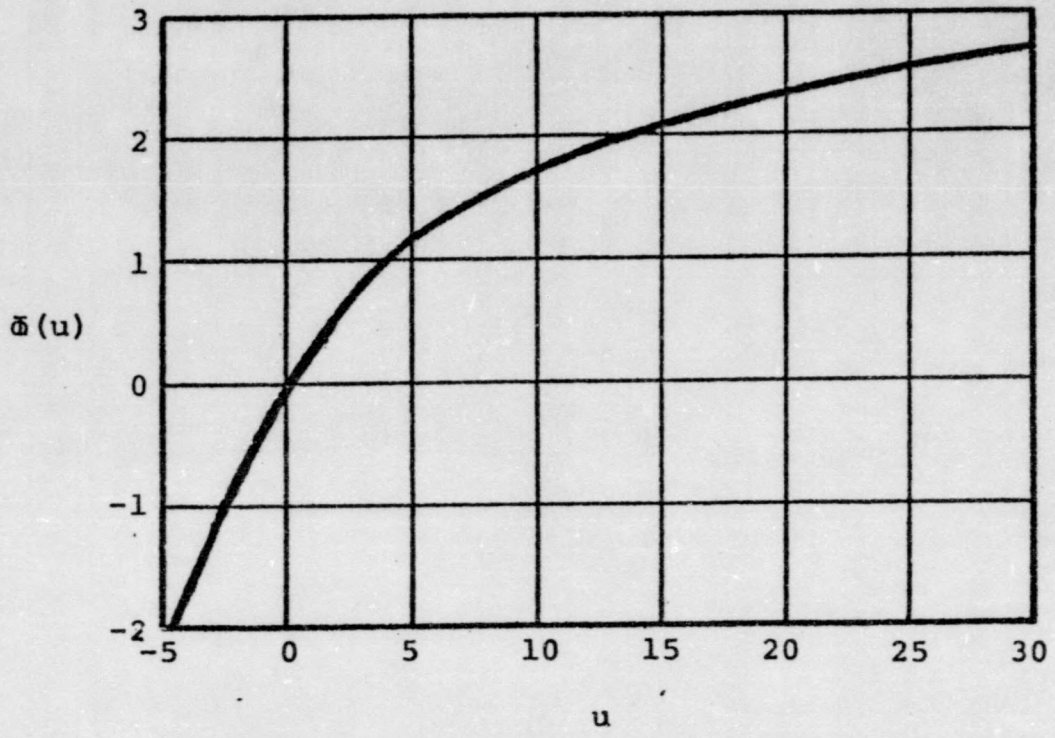

u	log |u|	Φ̄(u)	u	log |u|	Φ̄(u)
-5.0	0.699	-2.171	1.5	0.176	0.400
-4.0	0.602	-1.739	2.0	0.301	0.546
-3.0	0.477	-1.308	3.0	0.477	0.785
-2.5	0.398	-1.095	4.0	0.602	0.983
-2.0	0.301	-0.884	5.0	0.699	1.150
-1.5	0.176	-0.674	6.0	0.778	1.293
-1.0	0.000	-0.469	8.0	0.903	1.527
-0.5	-0.301	-0.268	10.0	1.000	1.713
-0.2	-0.699	-0.160	12.0	1.079	1.866
0.0	-∞	-0.085	14.0	1.146	1.998
0.2	-0.699	-0.015	16.0	1.204	2.113
0.4	-0.398	0.055	20.0	1.301	2.305
0.6	-0.222	0.125	25.0	1.398	2.497
1.0	0.000	0.249	30.0	1.477	2.655

The values of Fowler's function $\bar{\Phi}(u)$ and the theoretical curve are taken from DuBridge.[18]

Figure 3. Values for Fowler's Function, $\bar{\Phi}(u)$, and Fowler's Theoretical Curve, $\bar{\Phi}(u)$ versus u.

which emission may come -- from the top of the valence band; from acceptor and donor impurity states; from localized surface states; and from the bottom of the conduction band. Each of these levels has its own corresponding energy but, unless electrons reside at the Fermi level, they will not produce the work function.

The position of the Fermi level is dependent on the temperature and upon the amount of doping. Surface states, which result from doping (acceptor levels in cuprous oxide), produce a negative or positive surface charge giving rise to an electric field just outside the surface. From the theory of Gaussian surfaces, it is known that the surface charge distribution is compensated by a space charge underneath the surface. An electrostatic double layer of potential $U = - e V(x)$ is inferred from Poisson's equation. This potential is responsible for the band bending at the surface (see Figure 4). In the case of the surface being more P-type (figure 4a) than the bulk, the negative surface charge is due to the ionized acceptor states. If the space charge is large enough then the Fermi level might cut through the valence band (Figure 4b), resulting in an increase in the conductivity and the probability of electrons at the Fermi level. Similiar arguments can be made for N-type surfaces which bend downward (Figures 4c and 4d)[19].

Theories of photoelectric emission from semiconductors presented by Apker, et al[20] (1948) and Kane[21] (1961) predict a power law for the yield near the threshold

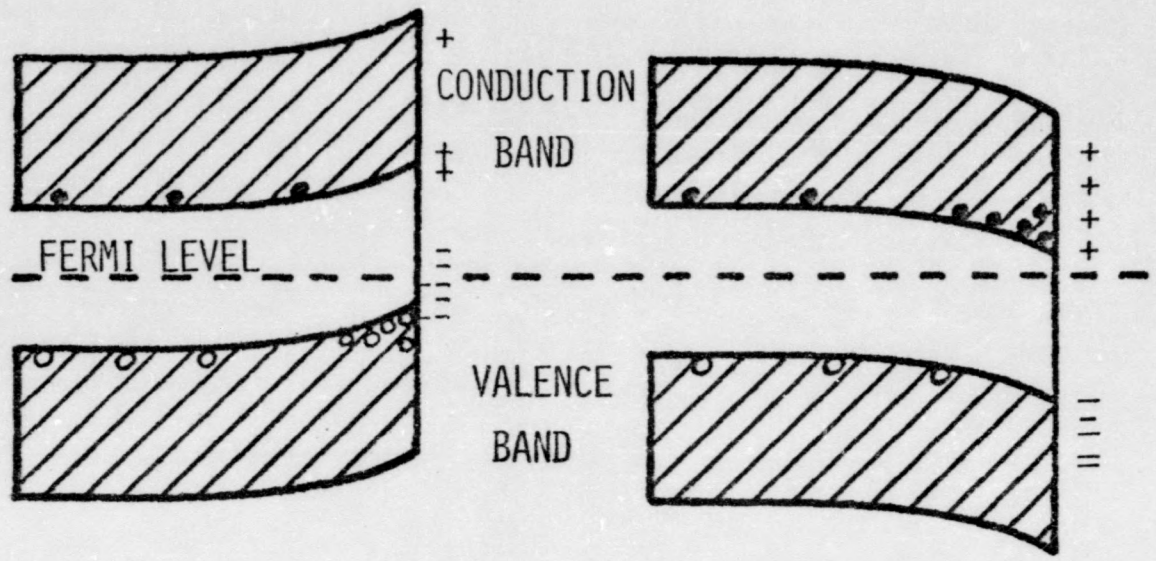

A. Surface more P-type.

C. Surface more N-type.

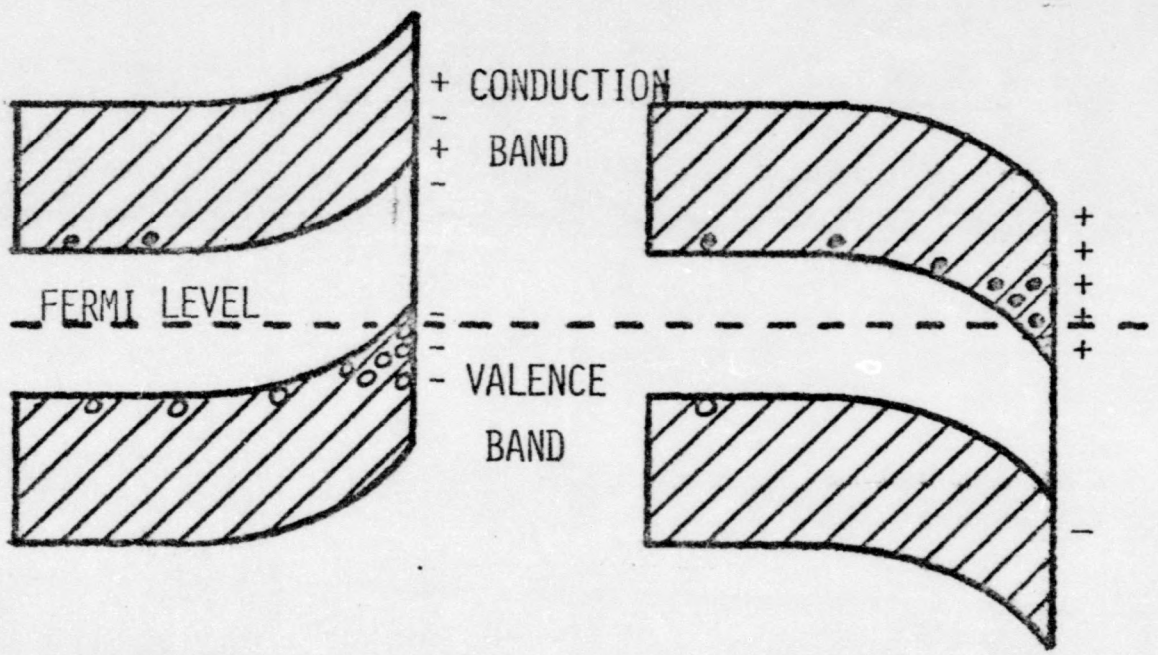

B. Degenerate P-type Surface.

D. Degenerate N-type Surface.

Figure 4. Band Bending at a Semiconductor Surface.

$$Y = C\,(h\nu - E)^{n}$$

where the exponent, n, depends on the excitation and escape mechanisms involved. Table 1 summarizes the mechanisms studied theoretically by Kane using the law of conservation of energy and momentum. Note that direct transitions occur between identical wave vectors in different bands. Allen and Gobeli[22] working on silicon, Spicer[23] working on alkali-antimonides, and Komp[8] working on cuprous oxide indicate that several mechanisms coexist to produce a composite yield

$$Y = A\,(E - E_o)^{m} + B(E - E_o)^{n} + \ldots\ldots$$

where one mechanism is likely to dominate. These investigators and Fischer[19] agree that the high yield threshold is due to direct transition of valence electrons. Fischer also investigated the effect of clean and of N-type surfaces contaminated with cesium. For clean surfaces the low threshold from impurity and surface states was well defined, but for contaminated surfaces, it was inaccurate due to band bending.

In studying cuprous oxide, Komp[8] found the high energy threshold to be quite insensitive to surface effects. Hence, the high energy threshold value of 5.09 eV for cuprous oxide should be the result of direct excitation with elastic scattering from the top of the valence band. Also, Komp indicates that the low energy threshold after argon

VOLUME PROCESSES	DIRECT OPTICAL EXCITATION	UNSCATTERED		$Y = (E - E_T)$
		ELASTICALLY SCATTERED		$Y = (E - E_T)^2$
	INDIRECT OPTICAL EXCITATION	UNSCATTERED		$Y = (E - E_T)^{5/2}$
		ELASTICALLY SCATTERED		$Y = (E - E_T)^{5/2}$
SURFACE PROCESSES	VOLUME STATES: SURFACE AS MOMENTUM ABSORBER	"ROUGH" SURFACE		$Y = (E - E_T)^{5/2}$
		PERFECT SURFACE		$Y = (E - E_T)^{3/2}$
	SURFACE BAND STATES	DIRECT OPTICAL EXCITATION	$E_T > \|E_F\|$	$Y = (E - E_T)$
			$E_T = \|E_F\|$	$Y = (E - E_T)^{3/2}$
		INDIRECT OPTICAL EXCITATION	$E_T > \|E_F\|$	$Y = (E - E_T)^2$
			$E_T = \|E_F\|$	$Y = (E - E_T)^{5/2}$
	SURFACE IMPERFECTION STATES	DISTRIBUTED IN ENERGY	$E_T = E_F$	$Y = (E - E_T)^2$
		LOCALIZED IN ENERGY BELOW E_F		$Y = (E - E_T)$

Table taken from E. O. Kane[21].

Table 1. Dependence of Photoelectric Yield, Y, on Photon Energy, E, near Threshold, E_T, for a Variety of Production Mechanisms.

bombardment approached a value between 0.45 eV and 0.50 eV below the high energy threshold. This indicates the position of acceptor levels above the valence band and corresponds closely to the values of acceptor energies cited by Wright[5] (0.4 eV) and by Fortin and Weichman[6] (0.3 eV to 0.6 eV).

Band Gap Width

The band gap of cuprous oxide has been measured experimentally through optical investigations. Cuprous oxide has a characteristic absorption edge at approximately 6000 Å which corresponds to a band gap of 2.1 eV. Figure 5 shows the energy diagram for optical and thermal transitions proposed by Garlick[24]. Reported values of the band width of cuprous oxide range from 1.9 eV to 2.4 eV. Table 2 shows the results of measurements of the band gap width in cuprous oxide. If 2.3 eV is accepted as the band gap and 5.1 eV is the energy of the top of the valence band, then the electron affinity is 2.8 eV. The electron affinity is the difference between the ionization potential and the energy gap; that is, the energy of the bottom of the conduction band relative to vacuum zero.

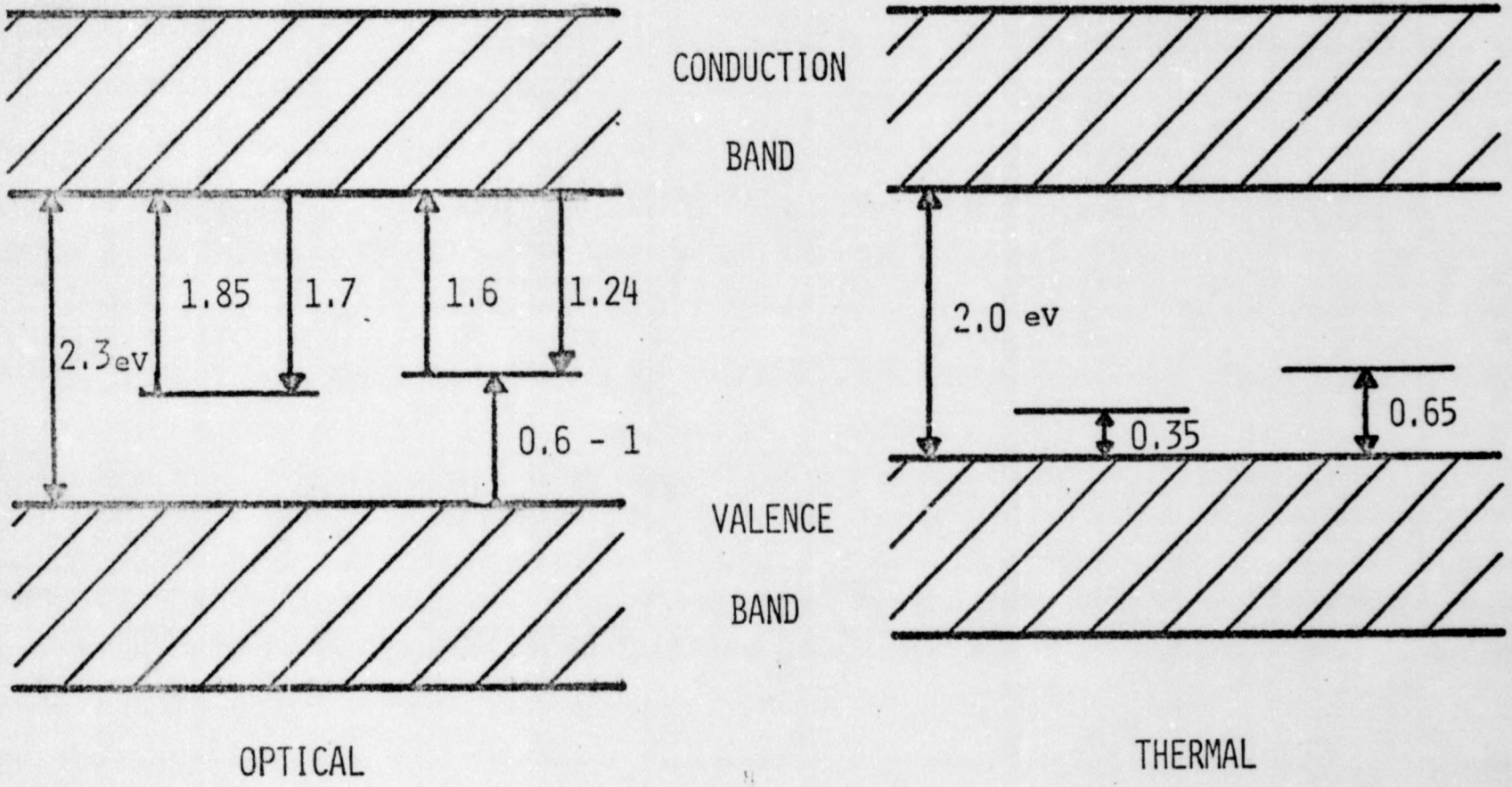

FIGURE 5. PROPOSED ENERGY-LEVEL DIAGRAMS FOR OPTICAL AND THERMAL TRANSITIONS.

AUTHORS	BAND GAP WIDTH (eV)	TYPE OF MEASUREMENT
Fortin and Weichman [6]	2.0	Thermo-conductivity
Dahl and Switendick [25]	2.38	Theoretical Calculation
Smirov [26]	2.3	Theoretical Calculation
Gross [27]	2.3	Optical
Zhilich and Makarov [28]	2.38	Theoretical Calculation
Smirov [29]	2.4	Theoretical Calculation
Brahms and Nikitine [30]	2.305	Absorption Spectra
Ioffe [31]	1.95	Optical

Table 2. Band Gap Measurements of Cuprous Oxide.

Previous Studies of the Work Function of Cuprous Oxide

Ioffe[9] made contact potential measurements of eleven cuprous oxide samples with respect to a gold reference using the ionization method. His value for the contact potential difference of cuprous oxide with gold is +0.05 ±0.04 eV where the work function of the gold reference was given as 4.76 eV without any reference to the experimental error. Thus, the work function obtained by Ioffe was 4.81 eV. More recent values of the work function of gold are above 5 eV[14].

Kuzel[32] has also measured the CPD of cuprous oxide with respect to a gold reference. In using the vibrating capacitator method, Kuzel found that the work function of cuprous oxide is slightly influenced by pre-illumination and by pre-heating of the samples. Illumination temporarily increases the work function of cuprous oxide. If cuprous oxide is illuminated by weak daylight for 2 - 5 minutes, the CPD is increased by as much as 15 mV. However, after 30 minutes the value returned to its initial value. Schick and Trivich[33] have recently studied the trapping mechanisms that are responsible for this "photomemory" effect in cuprous oxide.

Kuzel found that heating cuprous oxide samples to 250 °C did not greatly affect its work function. For samples heated to 130 °C, he measured the CPD to be 0.17 eV; samples

heated to 240 °C to 250 °C had a CPD of 0.07 to 0.09 eV; samples heated above 250 °C had a CPD of 0.03 eV. At temperatures above 250°C, the surface characteristics appear to have been altered; thus, samples should not be heated above 250°C.

THE EXPERIMENT

Sample Preparation

Cuprous oxide is prepared according to the method developed by Toth, et al [34] (1961). Oxygen free high conductivity copper 99.999% pure, is cut to approximate dimensions of 5 cm x 2 cm x 1 mm . A one-eighth inch support hole is punched in one end. Just before oxidation, the copper is etched in dilute nitric acid, rinsed in de-ionized water, and dried in air. While drying, a piece of Whatman #1 filter paper is touched to the water drop pendent from the bottom of the copper sheet.

When the sample is dry, it is lowered into a preheated vertical furnace. Three prongs protruding horizontally keep the sample and the three thermocouples (platinum -platinum + 13% rhodium) centered in the mullite furnace core. The three thermocouples are positioned at the center of the sample, 5 cm above and below the center, respectively. They are monitored manually using a selector switch on a Leeds-Northrup model 8691 potentiometer. The furnace is scanned vertically until the center thermocouple reaches the highest temperature. At this temperature the top and bottom thermocouples should read approximately the same temperature and should be within 10 °C of the center thermocouple. It is

improbable that the temperature gradient across the sample approaches this value because of the scanning technique used.

Oxidation of copper at 1020 °C and at atmospheric pressure requires about 5 hrs. To insure complete oxidation the sample remains in the furnace twelve hours. The temperature is then increased to 1085 °C to 1090 °C (the copper-cuprous oxide eutectic point is 1065 °C) and the crystal grows for three days.

The temperature of the furnace is monitored by a Honeywell strip chart recorder. The furnace and control were designed and constructed in this lab (see appendix 1 and 2). No deviations greater than 3 C at 1090 °C were recorded in a twenty-four hour period.

After three days the temperature is lowered to 1020 °C and the sample is equilibrated for two hours. Finally, the sample is withdrawn quickly to freeze in the proper stoichiometry. Note that samples annealed at 1020 °C and at atmospheric pressure are within the cuprous oxide stability region (Figure 1). Upon removing the sample from the furnace, it must pass through the cupric oxide, CuO, stability region. If this transition occurs quickly enough, only the surface (which can be removed) is affected. After the cupric oxide layers are removed, the diffusion of oxygen into the cuprous oxide occurs so slowly in air that short term aging effects are negligible.

Since the copper ions diffuse from the center to the surfaces, vacancies occur near the center of the sample. This imperfect region is removed by grinding through to the center with #320 grit alumdum and finished with #600 wet or dry silicon carbide paper. Methyl alcohol is used as a lubricant. The other surface is likewise ground parallel to the first until the cupric oxide layer is removed. The sample is then cut to approximate dimensions 3 cm x 2 cm with an X-acto knife. Finally, it is etched in 0.5 molar potassium cyanide and rinsed in de-ionized water. The sample is now placed in the vacuum system without further cleaning.

Analysis Of Samples

X-ray techniques, the powder method and the Laue method, were used to confirm the composition of and to orient the crystals, respectively. Photomicrographs of the crystal surface were taken with an optical microscope using transmitted light. Figure 6 gives the results of the powder method. The sample is indeed cuprous oxide. Figure 7 is a transmission Laue pattern showing that the crystal orientation of the samples is along the 3-fold axis, the (111) direction. The rings in the picture are characteristic of the apparatus; that is, identical rings were produced when no sample was used. The photomicrographs (Figures 8 and 9) show the typical surface conditions of the cuprous oxide samples. Grain boundaries are prominent. The

COMPOUND CUPROUS OXIDE RADIATION Mo KVP 50 mA 16

FILTER ZIRCONIUM LAMDA 0.71070 Å EXPOSURE 1 hr.

X_1	X_2	$I_{ex.}$	$D_{ex.}$	$I_{th.}$	$D_{th.}$	% ERROR	hkl
171.85	205.70	1 %	3.0136	9 %	3.020	0.21 %	(110)
168.00	209.60	100 %	2.4550	100 %	2.465	0.41 %	(111)
164.80	212.70	40 %	2.1346	37 %	2.135	0.02 %	(200)
154.50	222.80	30 %	1.5043	27 %	1.510	0.38 %	(220)
148.50	228.85	20 %	1.2834	17 %	1.287	0.28 %	(311)

D AND X ARE MEASURED IN mm.

FIGURE 6. POWDER DIFFRACTION ANALYSIS OF SAMPLE (Cu_2O).

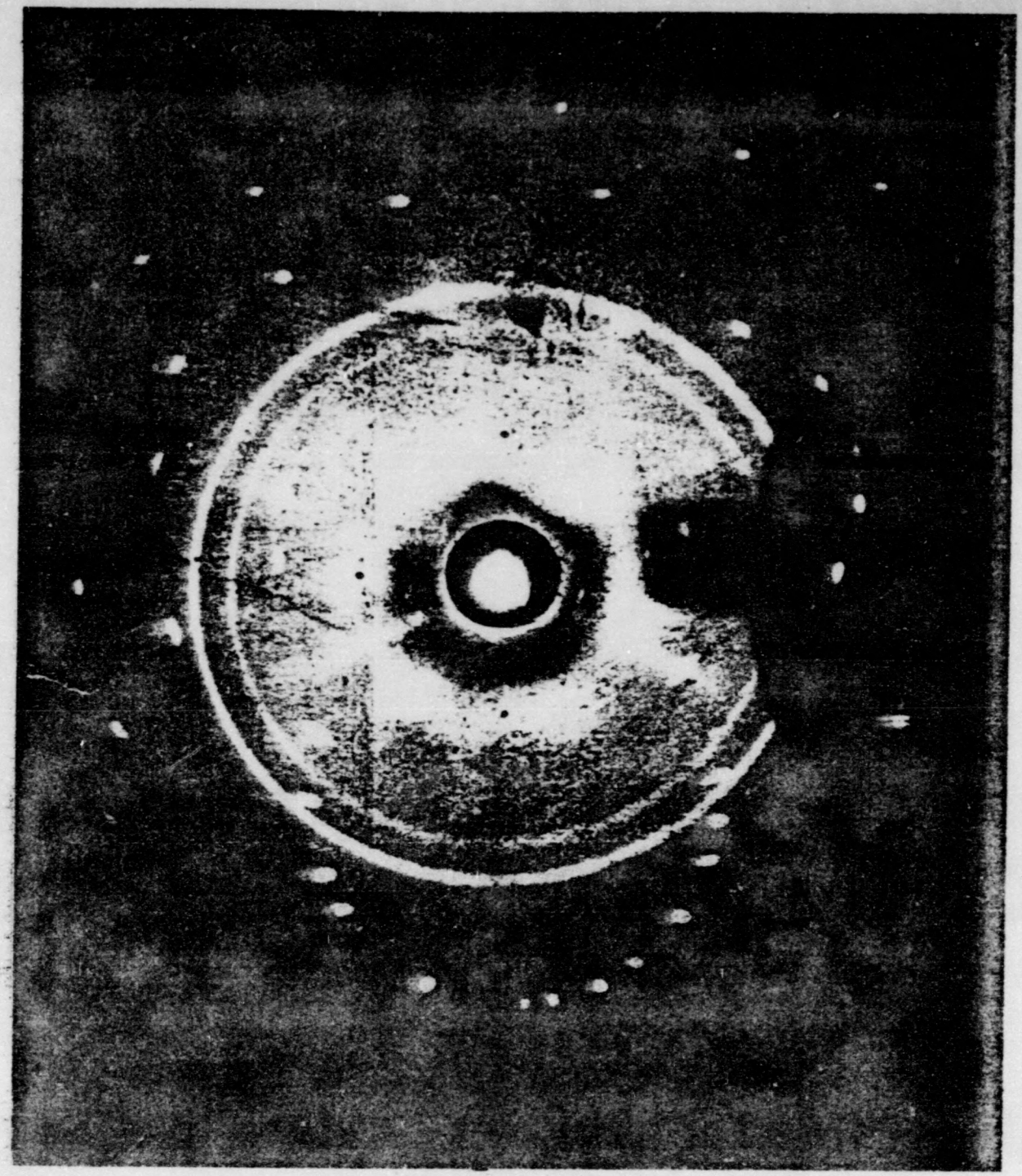

FIGURE 7. TRANSMISSION LAUE PATTERN FOR CUPROUS OXIDE.

FIGURE 8. PHOTOMICROGRAPH OF CUPROUS OXIDE SAMPLE (250 X).

FIGURE 9. PHOTOMICROGRAPH OF CUPROUS OXIDE SAMPLE (500 X).

slanted pyramids on the surface are faces of the crystal that are particularly resistive to attack by complexing etchants, KCN.

REFERENCE PREPARATION

Gold is evaporated on a glass microscope cover slide using a vacuum metalizing apparatus, CVE-14, constructed by the Consolidated Vacuum Corporation. This system, pumped by an oil diffusion pump and a mechanical roughing fore pump, attains pressure of magnitude 10^{-6} to 10^{-7} torr. The gold is evaporated on one side of the slide only. After depositing the gold on the glass slide, it is placed in the vacuum system.

Apparatus and Instrumentation

Vacuum System

CPD measurements as well as photoemission measurements must be undertaken in an ultra high vacuum because the absorption of gases effects these measurements. In addition, the operation of the electron gun requires a vacuum. The bakeable, all-metal ultra high vacuum system

(Figures 10a and 10b) is equipped with a standard size Varian VacSorb zeolite molecular sieve forepump and a Varian model 921-0013, eight liter VacIon pump. Figure 11 shows a simplified cross-section of the vacuum system through the center line of the ports.

Four stainless steel sample holders approximately 3 cm x 2 cm (Figure 11) are suspended and electrically insulated from the grounded system by a pyrex glass tube. The glass tube is connected to a Varian model 954-5120 positive drive rotary feedthrough which is capable of manually rotating the sample through angles greater than 360^{o} in vacuo by means of an external "wobble stick". During experiments, two cuprous oxide samples and a gold reference are clipped in the holders. The fourth holder remains empty. A single wire, common to the four sample holders, leads to the exterior of the vacuum system through an insulating seal. This lead is connected within a netic-conetic shielded box to a coaxial cable which is passed through a grounded copper tube to a Victoreen model 475 Dynamic Capacitator Electrometer. The copper tube not only acts as a shield but also keeps the cable stationary. The impedance of the electrometer is adjustable: 10^{10} ohms is used for contact potential difference measurements and 10^{12} ohms is used for photoemission experiments. The voltage drop across the input impedance is compensated for by a feedback circuit within the electrometer.

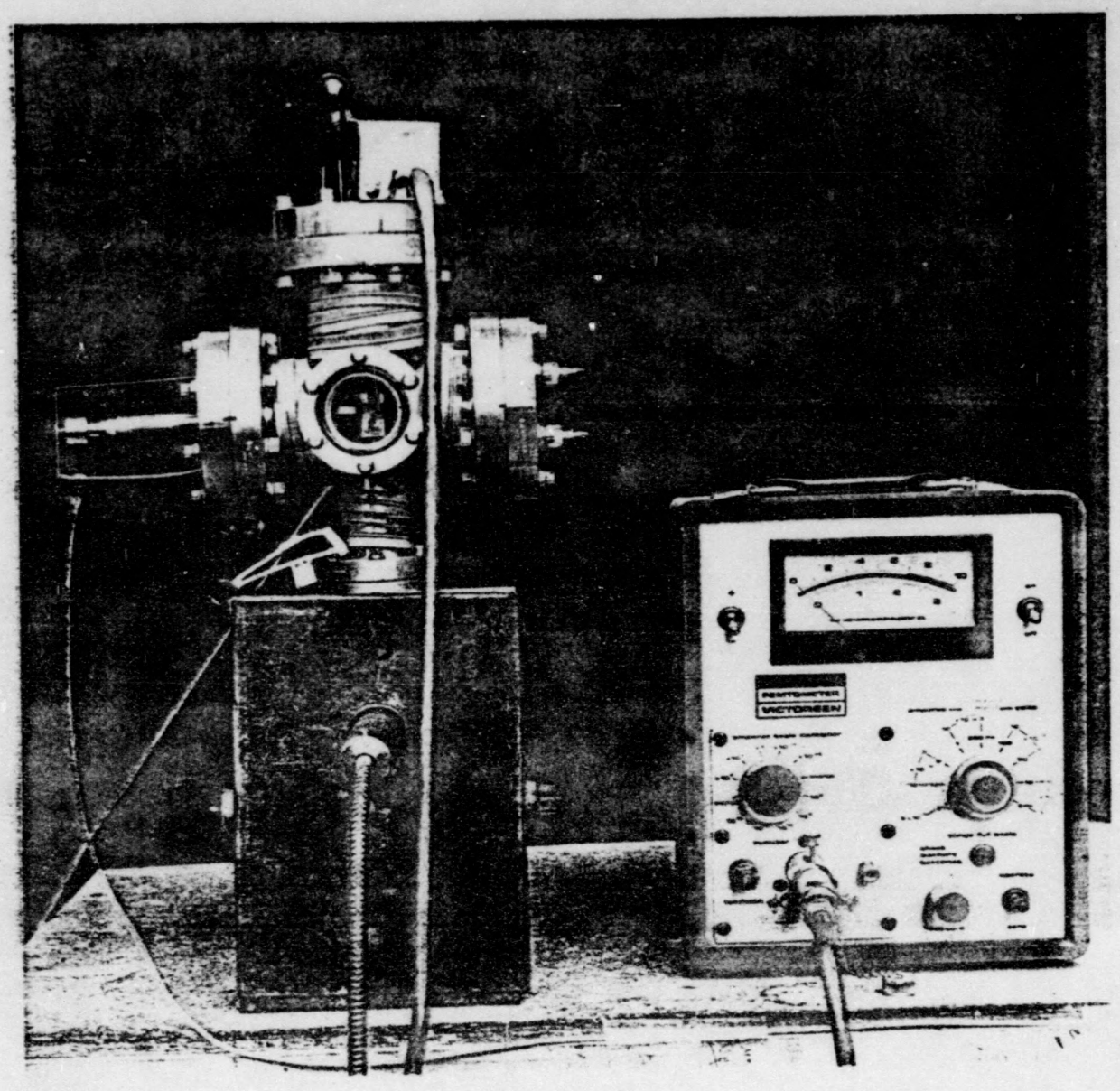

FIGURE 10A. THE VACUUM SYSTEM AND INSTRUMENTATION.

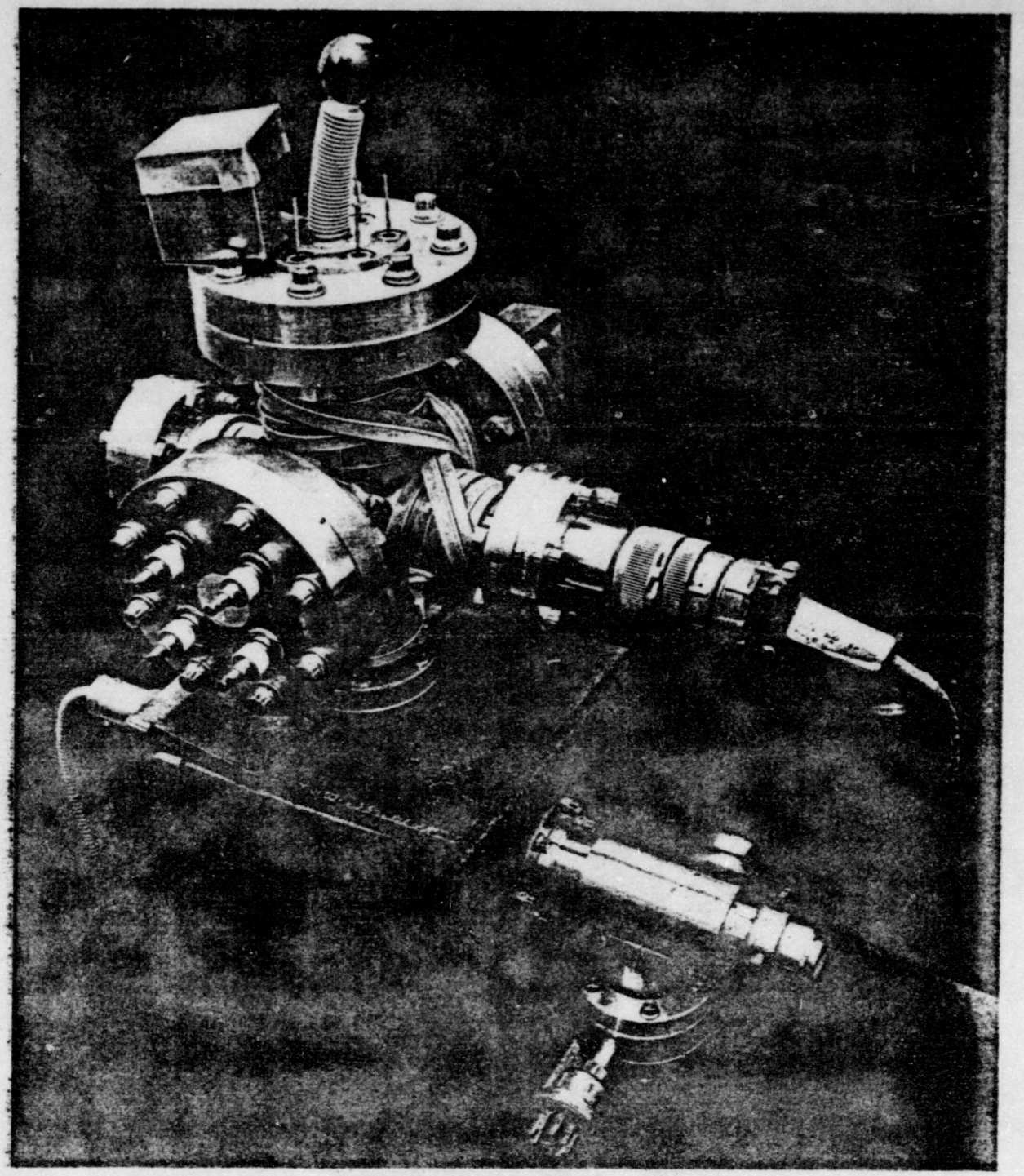

FIGURE 10B. THE VACUUM SYSTEM.

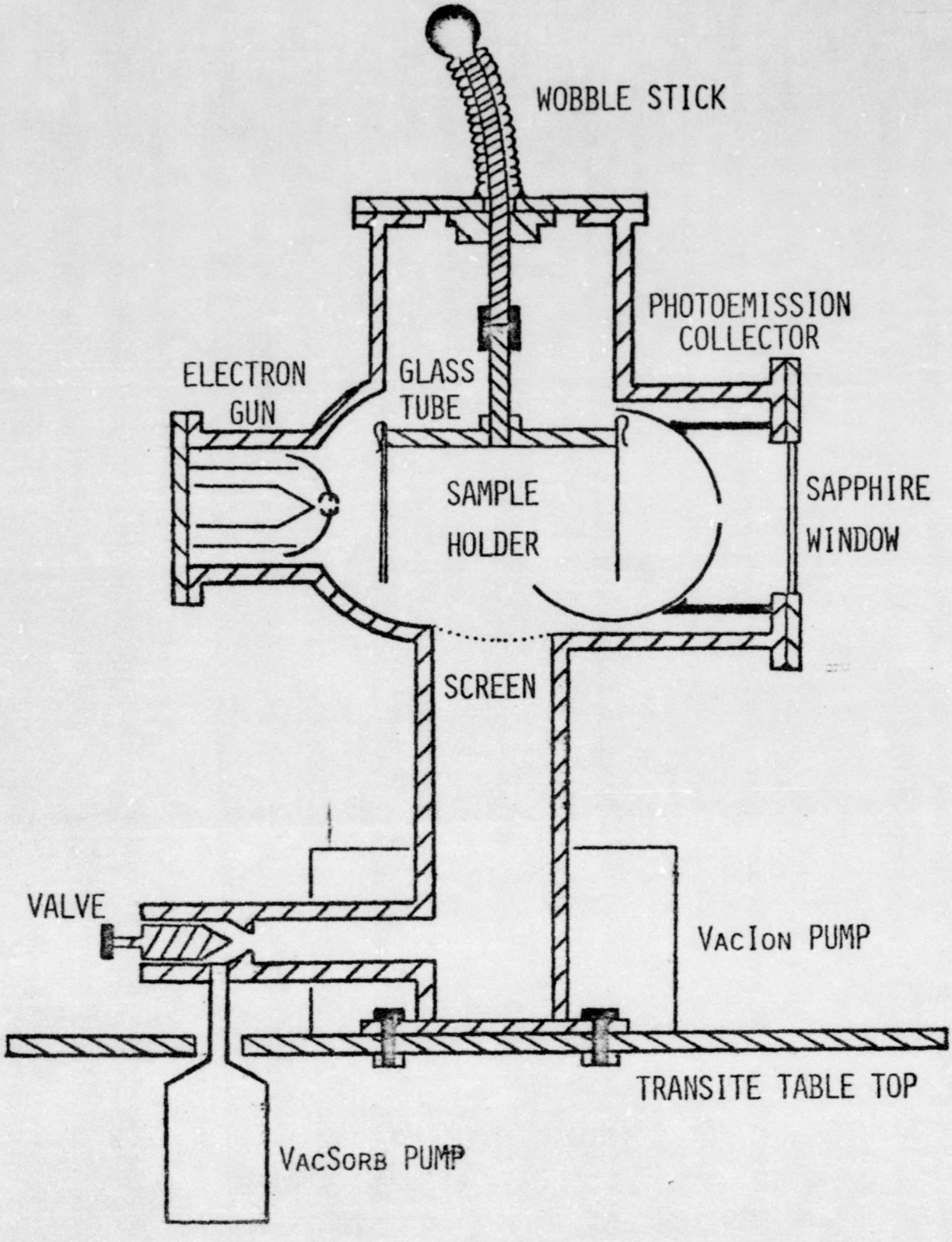

FIGURE 11. VACUUM SYSTEM CROSS-SECTION.

The bakeable vacuum system is bolted to a transite table with the absorption pump protruding beneath the table top. In order to clean the absorption pump, it is heated by a 260 watt heater cartridge for a twenty-four hour period with the pump open to the atmosphere. This treatment expells much of the absorbed gases, especially water vapor (a polar molecule that will influence the properties of the surface). Then the system is closed to the atmosphere and the valve between the sample chamber and the roughing absorption pump is opened as the absorption pump is cooled with liquid nitrogen. Generally, at this point, the sample chamber is heated with a heating tape wrapped around the system. A variac maintains a temperature below 100°C. Note that the cuprous oxide sample is not thermally insulated from the system and therefore, the system cannot be heated above 100°C . At temperatures above 100 °C the stoichiometric ratio changes and thus the properties of cuprous oxide change. Realizing the possible effects of heating cuprous oxide to this temperature, the last two samples were not subjected to this treatment. When the absorption - desorption process reaches an equilibrium (usually in the 10^{-2} torr region), the valve between the absorption pump and the sample chamber is closed and the VacIon pump is started. The system is allowed to bake for twelve hours. In the throat of the port leading to the VacIon pump is a grounded screen which reduces the ion current reaching the sample.

Typical pressures produced in this manner are of the order of 10^{-7} torr.

Electron Gun

A cross-section of the electron gun is shown in Figure 12 and a schematic of the gun control is shown in Appendix 3. The gun control panel and the X-Y Recorder are shown in Appendix 4. The potential of the filament tip that is aligned with a 0.003 in. collirated orifice in the hemispherical anode is adjusted to gun potential by the potentiometer. Electrons emitted from the tungsten filament operated at 1.5 V a.c. and 40 mA are accelerated towards the anode by a 2 V field. The cylindrical shield is maintained at a negative 5 V with respect to the gun potential. The gun potential is varied with respect to the sample by a Lambda model LS-511 10 V d.c. Precision Power Source. The entire sample chamber and gun are shielded against magnetic fields by netic and conetic shields. As previously indicated, the current through the sample is monitored by a Victoreen electrometer. The amplified output (0 to 30 V full scale) of the electrometer is fed into the Y-axis of a Hewlett-Packard model 7004A X-Y recorder. The X-axis monitors the gun potential; that is, the bias of the Lambda power supply.

A space charge around the filament will result from operating the anode at a positive 2 V. This tends to

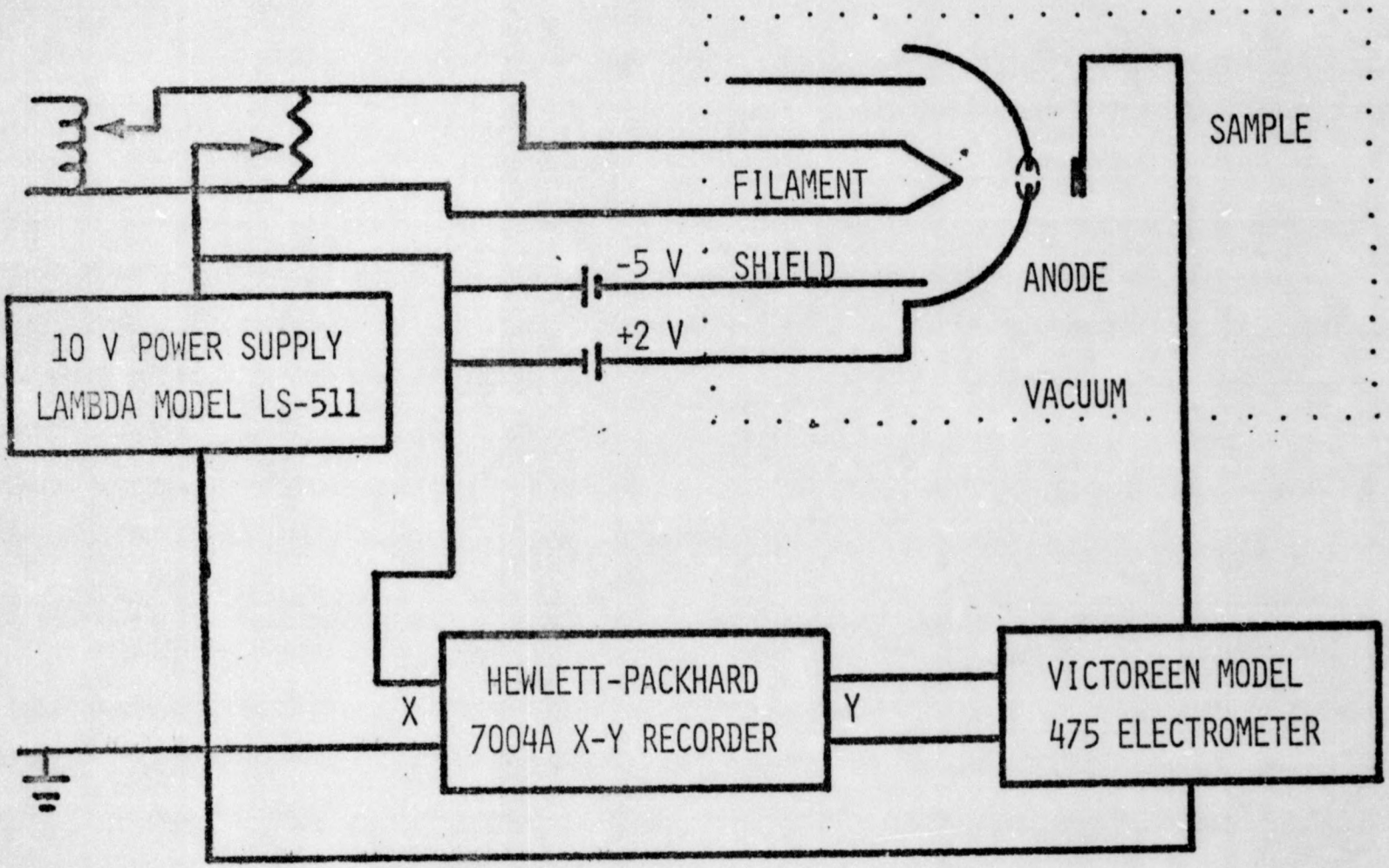

FIGURE 12. ELECTRON GUN CROSS-SECTION AND INSTRUMENTATION.

lower the apparent work function of the filament and produces a work function characteristic of the gun rather than of the filament. The advantage of operating the gun at space-charge limited potentials is that the non-uniformity in the field produced between the sample and the anode, is negligible. If the anode is operated at 15 V (Nelson[11]) then a more non-uniform field results.

Photoelectric Emission From Gold

The work function of the gold reference is found by photoelectric emission experiments undertaken with the apparatus shown in Figure 9. Light from a Hanovia medium pressure mercury lamp is passed through a 150 mm Hilger and Watts monochromator. Since the work function is known to be in the range of 5 eV, the wavelength of light with sufficient energy to cause emission would be less than 2500 Å.

In order to calibrate the monochromator, light from the monochromator is projected on a sodium salicylate window. When ultra violet light shines on sodium salicylate it fluoresces in the visible with an intensity proportional to the number of photons that strike it, independent of the wavelength (in that region of the uv). The visible light signal is detected and amplified by a RCA 1P21

photomultiplier, operated at 400 V d.c. supplied by a Kepco supply. The output is amplified and input in the Y-axis of the Hewlett-Packard X-Y recorder while the X-axis monitors the wavelength. A gear mechanism and a 500 ohm, 10 turn potentiomenter are used to produce a voltage proportional to the wavelength. The monochromator is calibrated by comparing the wavelength and the intensity of the peaks with the published, standard mercury lines. Appendix 5 shows the calibration curve.

In the experiment, light from the monochromator is collimated by two aluminium sheets with a one-eigth in hole. The light emerges from the sapphire window; traverses the vacuum; passes through the hole in the collector and strikes the sample (Figure 13). The collector, operated at a positive 100 V, is a spherical glass shell, somewhat larger than a hemisphere. Its interior is coated with alca dag. When light of sufficient energy falls on the gold, the emitted electrons are accelerated toward the collector and the electrometer indicates a current.

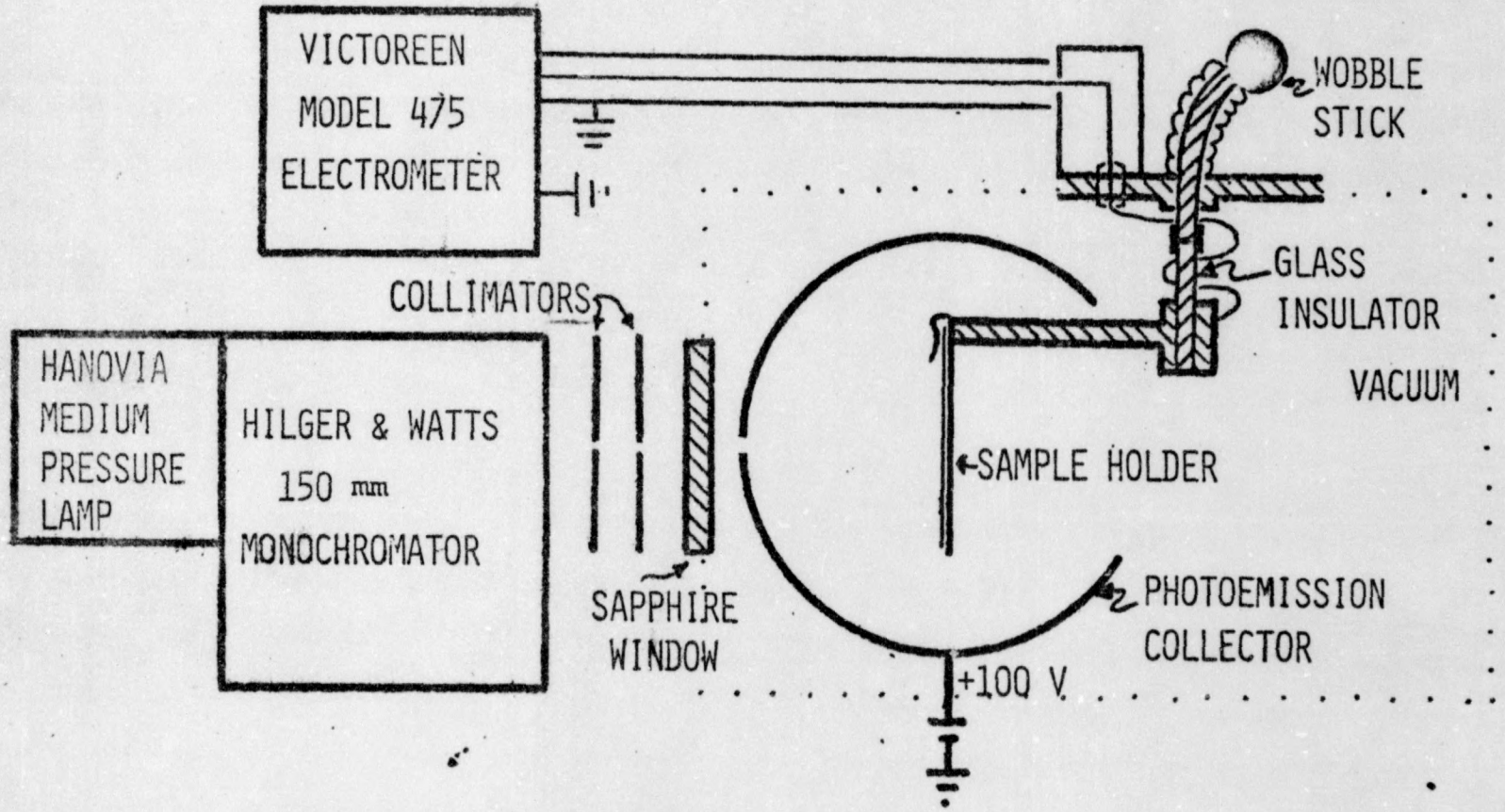

FIGURE 13. INSTRUMENTATION FOR PHOTOEMISSION EXPERIMENTS.

EXPERIMENTAL RESULTS

The Procedure

Four cuprous oxide samples were subjected to a similiar experimental program which is outlined below. Each of these samples, designated by "D", "Z", "G", and "S", were grown at 1085 C and equilibrated at 1020 °C.

1. The VacSorb pump is cleaned by heating overnight. Then it is isolated from both atmosphere and the sample chamber.

2. The sample is placed in the vacuum system. The first set of experiments was undertaken with two samples (D and Z) and two gold references; the second set of experiments was undertaken with two samples (G and S), one gold reference, and a stainless steel control. All contacts were ohmic.

3. The vacuum system is closed to the atmosphere and the valve between the sample chamber and the VacSorb pump is opened. The pump is cooled with liquid nitrogen. After an equilbrium pressure is reached (approximately 10^{-2} torr) this valve is closed and the VacIon pump is turned on. Pressures of 10^{-7} torr result.

4. At this point the sample chamber is heated in the first experiment (samples D and Z) but not for the second experiment (samples G and S).

5. The preliminary procedure is the following:

The gun control is turned on. The filament is adjusted until the anode current reads 10^{-6} A. A few minutes is allowed for the anode current to stabilize. Initially, the anode current drifts erratically but it becomes stable after a few minutes. When the anode current is stable, one of the samples is turned by the "wobble stick" until it is aligned with the gun.

6. The experiment proceeds as folows:

a. A point plot of the cuprous oxide sample electron beam current (Y-axis) versus the gun potential (varied manually) is made by manually depressing the pen bar at 0.1 V intervals.

b. Similarly a point plot of the gold reference is superimposed on the same graph. Since the two plots are almost identical they are offset vertically.

c. The horizontal shift between the two plots; that is, the CPD, is found graphically by determining the potential difference between the two peaks.

7. After the CPD measurements are completed, the work function of the gold reference is found by photoelectric

emission experiments. These measurements are conducted as follows:

a. The Hanovia lamp is allowed to warm up. During this period the X-axis is connected across the center of a 10-turn potentiometer. The potential is varied proportional to the wavelength by a gear mechanism. The Y-axis records the 0 to 30 V full scale output of the electrometer whose input impedance is set at 10^{12} ohms.

b. The room is then darkened; the slit of the monochromator is opened, and a plot of the sample current versus the wavelength (2000 $\mathring{A}$ to 3000 $\mathring{A}$) is made.

c. The plots are analyzed according to Fowler's theory.

Discussion of the Results

Preliminary experiments showed that cuprous oxide and gold had approximately the same work function. In the preliminary experiments, it was noted that the anode current drifted. This did not shift the plot horizontally although the slight vertical drift, when it occurs at the peak, makes it difficult to locate the maxima. If the experiments are performed quickly enough; that is, within a few volts of the peak, these drifts could usually be eliminated and a smooth peak would result.

The data taken is consistently reproducible. CPD data curves for the four samples are given in Figures 14 through 17 and Table 3 summarizes the results. The limits on the error were assigned a value of ±0.05, one-half the horizontal interval between points on the curve.

Several differences in the early measurements on samples D and Z from the measurements made on samples S and G are observed. First, the electron beam current of the latter experiments is an order magnitude greater than that of the earlier experiments. This is attributed to a better alignment of the filament with the orifice in the anode. If the sample "sees" a part of the filament other than the tip, then the electron could come from the space charge around the tip or from another part of the filament which would be at a lower potential than the tip. Hence, the apparent work function of the gun will vary with different filament alignments. However, as long as the work function of the gun remains constant during the measurement, then the CPD, although shifted relative to gun potential, will be a constant.

In the first experiments, the position of the peak with respect to the gun potential occured at a potential of greater than - 1.0 V; the position of the peak in the latter experiments was approximately - 3.0 V. If the work function of the gun is a constant during the experiments, it does not enter into the calculation of the CPD because both the sample curve and the reference curves are shifted by the

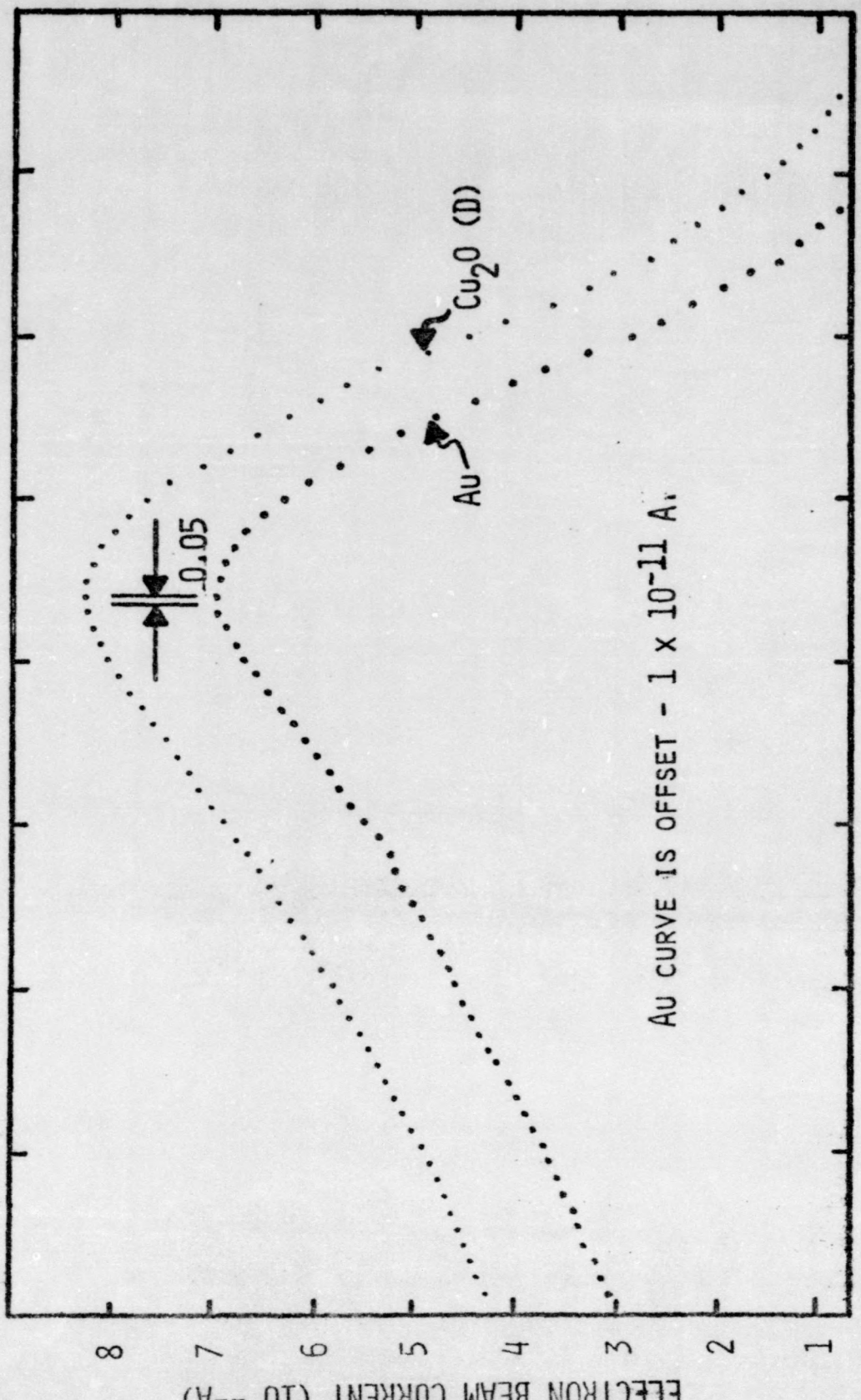

FIGURE 14. CUPROUS OXIDE (D) DATA CURVE.

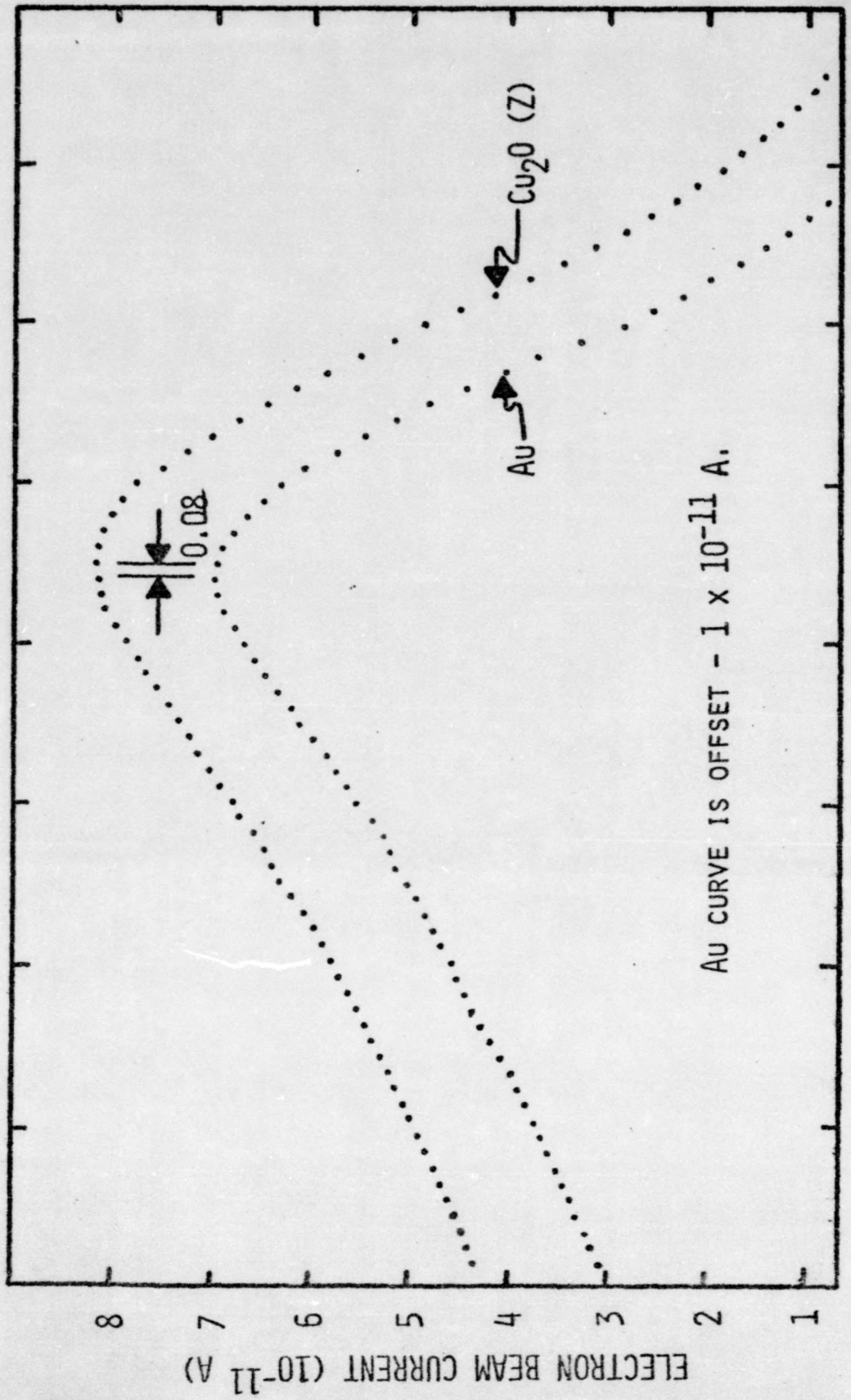

FIGURE 15. CUPROUS OXIDE (Z) DATA CURVE.

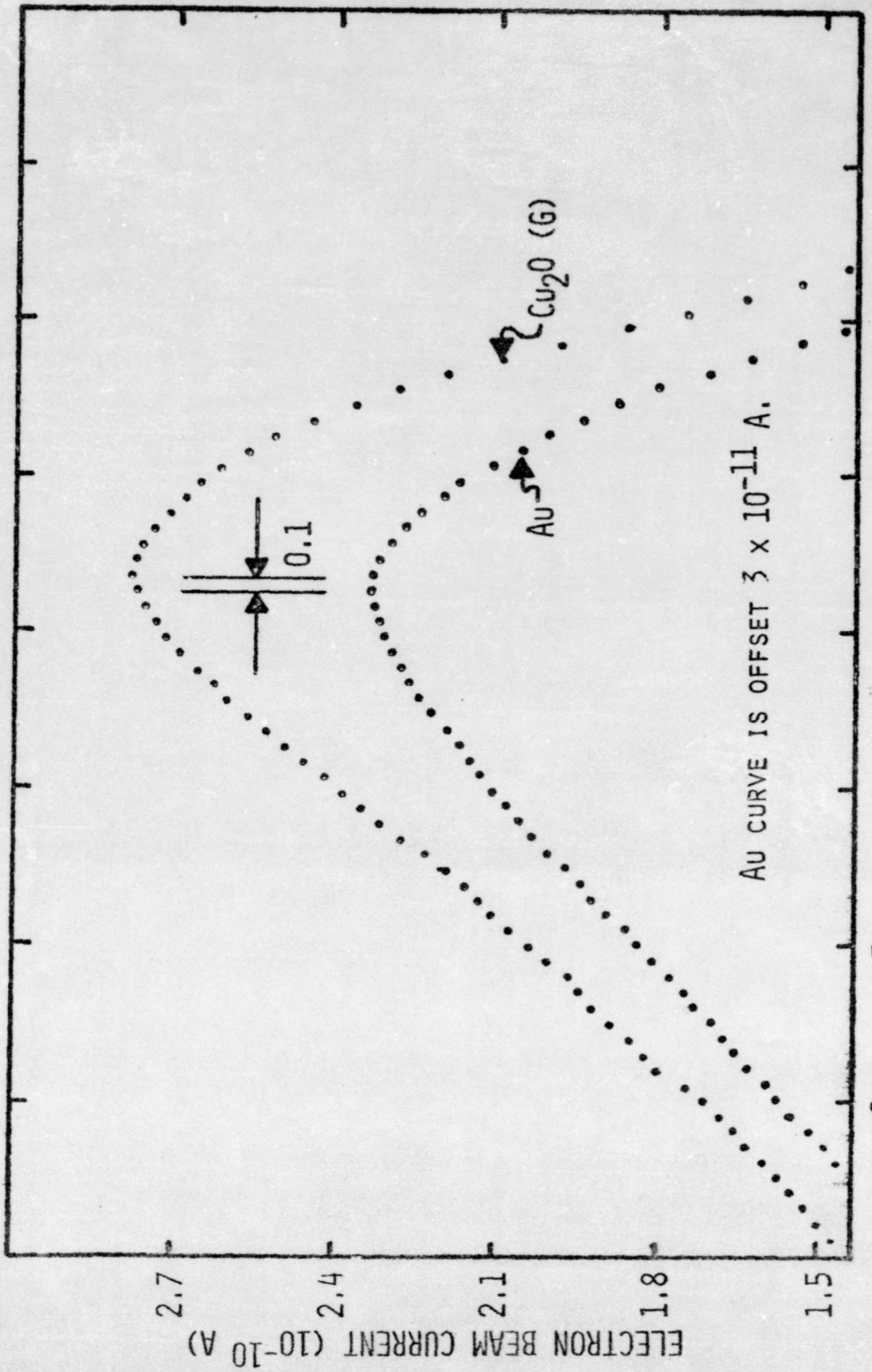

FIGURE 16. CUPROUS OXIDE (G) DATA CURVE.

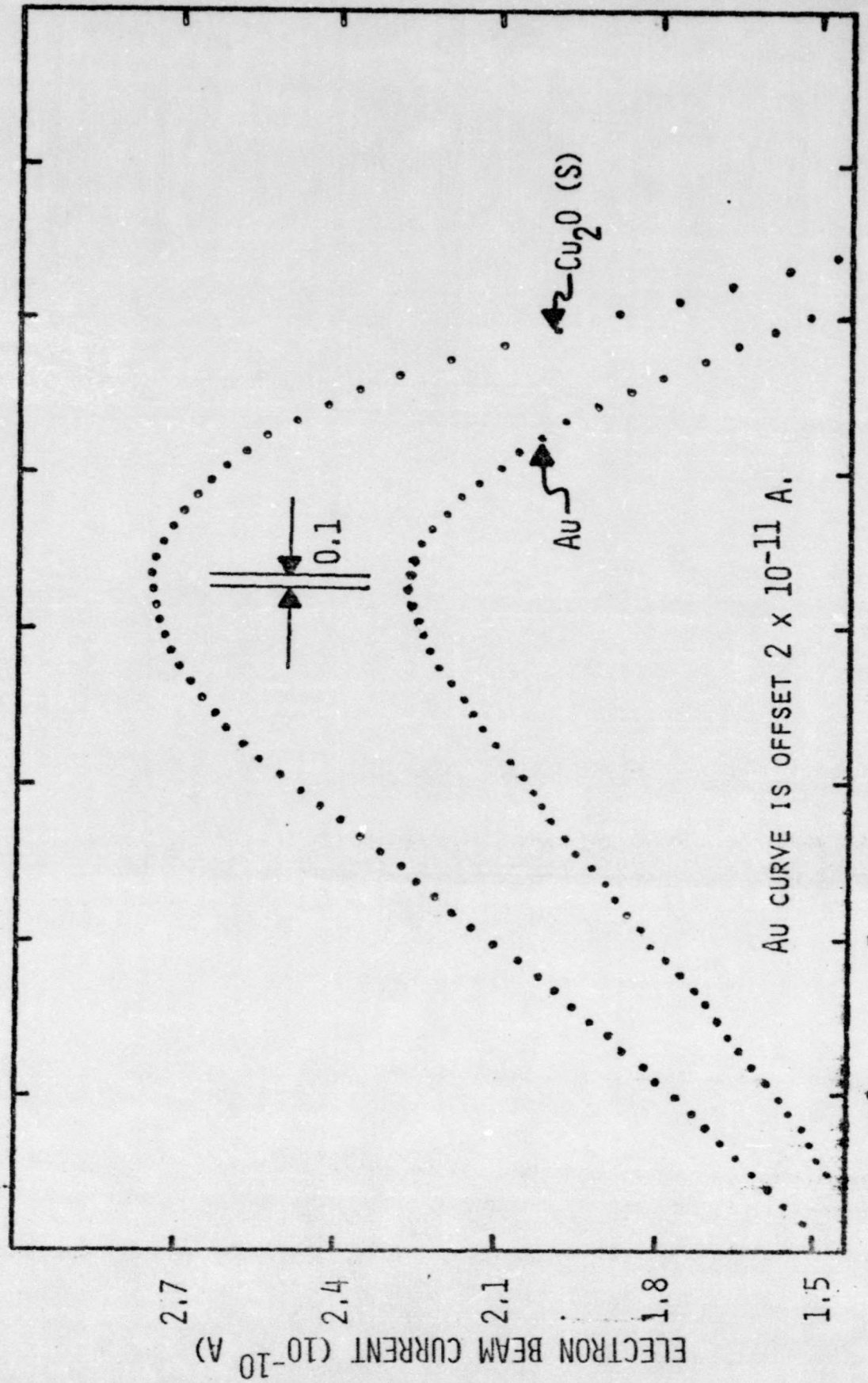

FIGURE 17. CUPROUS OXIDE (S) DATA CURVE.

SAMPLE	CPD WITH RESPECT TO GOLD (eV)
Cu_2O (D)	0.05 ±0.05
Cu_2O (G)	0.1 ±0.05
Cu_2O (S)	0.1 ±0.05
Cu_2O (Z)	0.08 ±0.05

TABLE 3. CPD MEASUREMENTS FOR THE FOUR SAMPLES.

same constant potential. As the data shows, the measurements are within experimental error of each other.

The fact that the second experiments made on samples S and G are consistently higher is attributed to band bending. The amount of band bending, and consequently, the work function, depends on the concentration of the absorbed species. In general, the greater the contamination, the lower the work function will be, because the Fermi level is shifted upward relative to vacuum zero.

The gold references were plated and the samples Z and D were grown more than six months prior to experiments. They were subjected to air for several months and were not re-etched before measurements were taken. The samples S and G were grown a few weeks prior to use and were etched only minutes before being placed in the vacuum system. Thus, it would be expected that the samples S and G would exhibit a higher work function. Since the same gold reference is used in all the experiments, the CPD of samples S and G should be greater.

As shown in Table 4, the CPD of the contaminated samples and the fresh samples are within experimental error of one another. Hence, it is concluded that cuprous oxide is not greatly affected by aging.

In addition, samples D and Z were heated to approximately 100°C; samples G and S were never heated above room temperature. If Kuzel's measurements are accurate, then the variation of the CPD due to temperature effects

would be within the experimental error of this experiment. This experiment can only indicate that the dependence of the work function on the thermo-history of the sample is within the experimental error (0.05 eV) for temperatures less than 100°C.

The CPD of cuprous oxide with respect to gold is on the order of 0.1 ±0.05 eV. Therefore, the work function of cuprous oxide is greater than that of gold. The CPD of the stainless steel control is approximately -0.1 ±0.05 eV with respect to gold; its work function is less than the work function of gold. If the work function of the gold reference were known, the work function of both the stainless steel and the cuprous oxide could be calculated.

Because of the low yield at short wavelengths from the 150 mm monochromator and the Hanovia lamp, photoemission experiments failed to produce the exact values for the work function of gold. The weak photoemission observed at 2300 Å coupled with the absence of photoemission from the strong 2536 Å mercury line indicates that the work function of the gold reference is above 4.9 eV. This means that the work function of cuprous oxide is approximately 5.0 ±0.1 eV.

CONCLUSIONS

From the work presented here, it can be concluded that the work function of cuprous oxide is larger than the work function of gold by 0.1 ±0.05 eV. This value agrees well with the CPD measurements presented by Kuzel (0.17 eV) and by Ioffe (0.05 ±0.04 eV). Since photoemission experiments indicate that the gold reference has a work function of about 4.9 eV, then the work function of cuprous oxide would be approximately 5 eV. This places the Fermi level at 5 eV above vacuum zero.

According to the measurements of the high energy threshold of cuprous oxide made by Komp (5.09 ±0.05 eV) and by Ioffe (5.15 eV), the position of the top of the valence band is about 5.1 eV above vacuum zero. In addition, the position of the acceptor levels above the valence band in cuprous oxide has been investigated by Wright (0.4 eV), by Komp (0.45 - 0.5 eV), and by Fortin and Weichman (0.3 - 0.6 eV). Thus, as predicted, the Fermi level resides between the valence band and the acceptor levels.

From optical measurements, the band gap has been determined to be 2.3 eV. Therefore, the electron affinity of cuprous oxide is approximately 2.8 ev. Figure 18 shows the proposed energy level diagram for cuprous oxide.

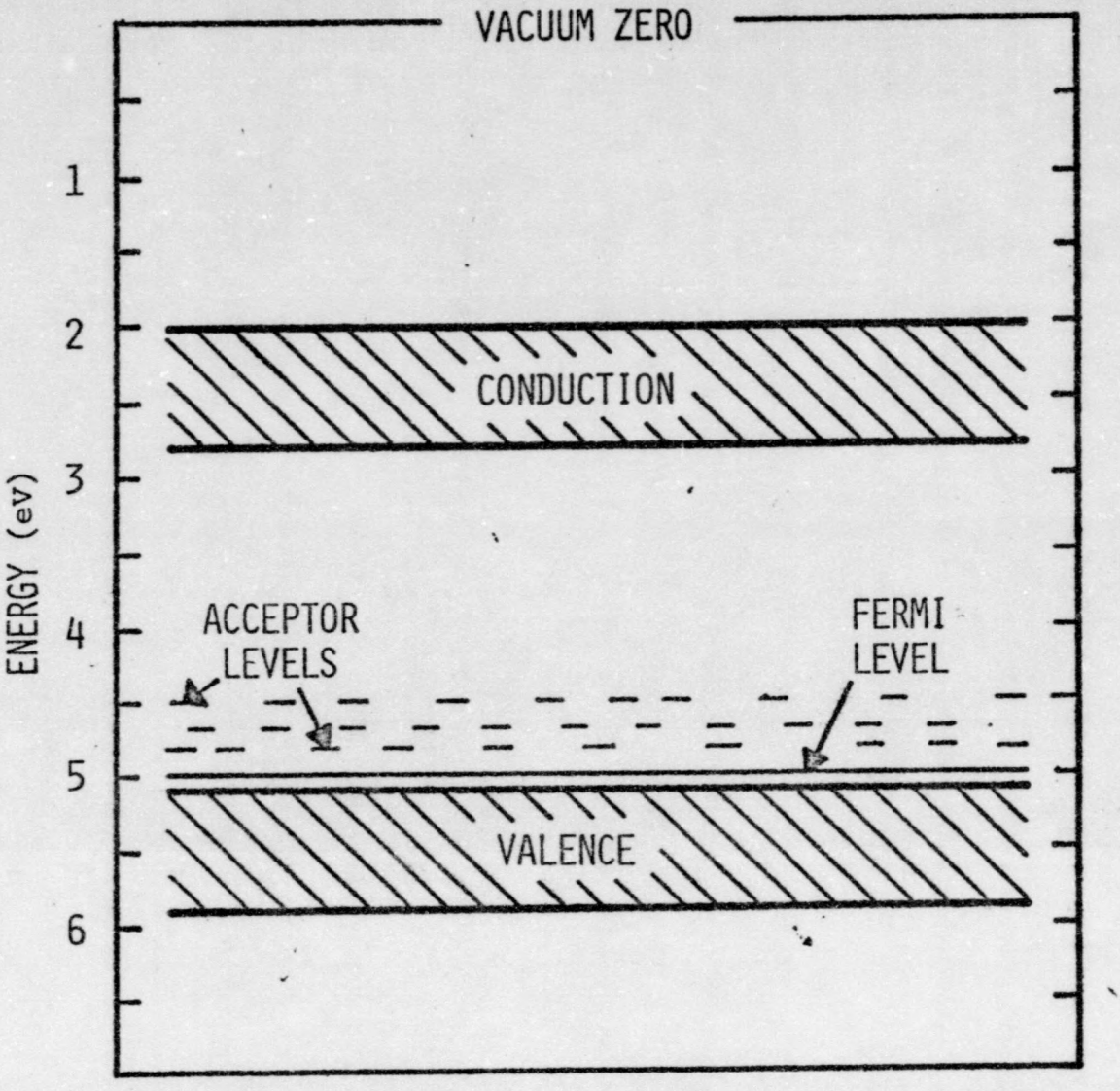

FIGURE 18. BAND STRUCTURE OF CUPROUS OXIDE.

The number of carriers in cuprous oxide is given by Kotsyumakha, et al.[35] to be of order the magnitude of 10^{12} holes/cm^3. Since the conductivity varies as the one-eigth power of the oxygen partial pressure, the number of carriers will vary little from sample to sample if precautions are taken to maintain the stoichiometry. If there are 10^{12} holes per cm^3, then the number of acceptor sites in cuprous oxide can be found by

$$N \text{ (holes)} = N \text{ (acceptor states)} \exp(-(EA - \emptyset)/kT)$$

where N (holes) is the hole concentration; N (acceptor states) is the number of acceptor states, and EA is the energy of the acceptor levels relative to vacuum zero. From Figure 14, the difference (EA - $\emptyset$) is 0.3 eV. The value of the exponential term at room temperature (300°K) would be 9.1×10^{-6}. This indicates that there are 10^{17} copper vacancies (acceptor states) per cm. From known values of the molecular weight of cuprous oxide (143.08 g/mole) and the density of cuprous oxide (6.0 g/cm^3), the number of molecules per cm^3 is calculated to be 2.5×10^{22} cuprous oxide molecules /cm^3. Since there are two copper ions per cuprous oxide molecule, there are 5×10^{22} copper ions per cm^3. There would be 2 ppm copper vacancies. This calculation compares well with estimates proposed by Bloem.[24]

Need for Further Study

Although the aging of the samples and the heating of the samples to 100 ^{o}C did not appear to influence the work function, more rigorous experiments are necessary to verify these conclusions. Also, since the cleaning of the sample in vacuo was ignored in this work, future studies should encompass a method of cleaning the sample in vacuo; such as, argon bombardment. By studying a sample before and after bombardment with argon, the effect that surface contamination and band bending have on the work function could be measured.

Even though all of the contacts were ohmic, there exists a contact potential difference at every contact. In this study, no attempt was made to determine how these contact potentials effect the experimental results. If the metallic contacts on the sample holder were replaced with metals of different work functions, the effect of these contact potentials on the measurements could be observed. Future studies should include such a study.

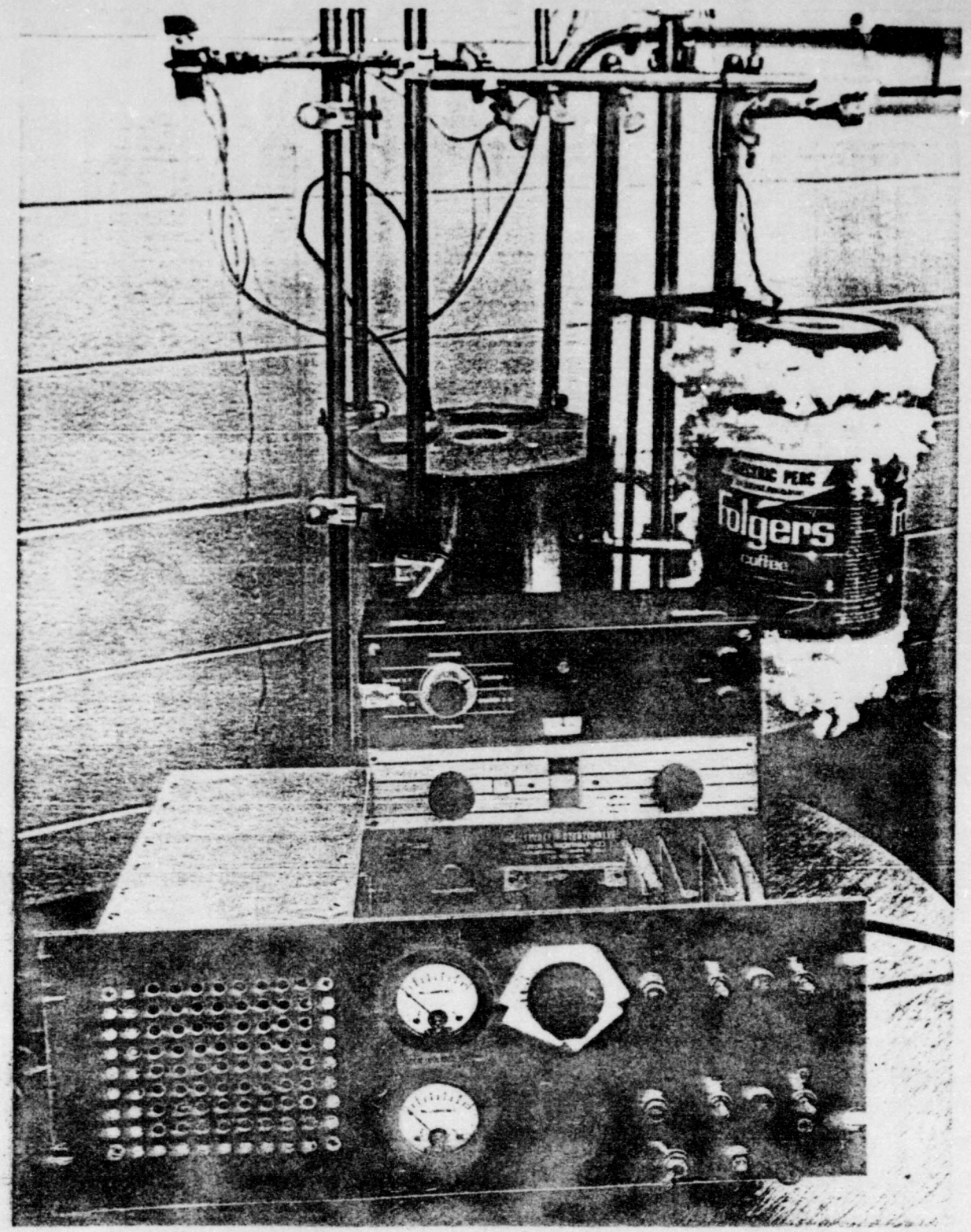

APPENDIX 1. SINGLE-ZONE AND TWO-ZONE FURNACE, FURNACE CONTROLLER, AND MILLIVOLT POTENTIOMETER.

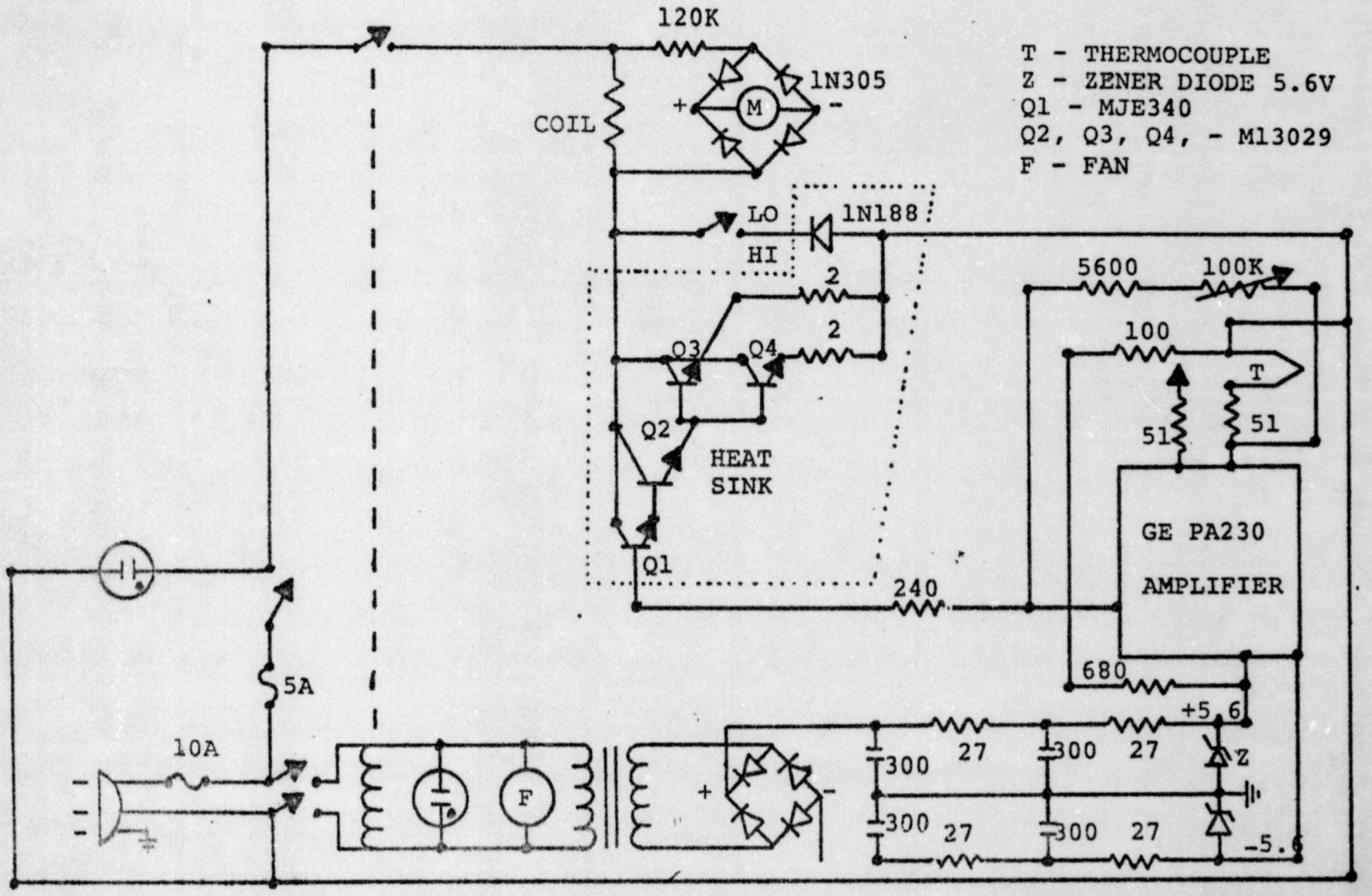

Appendix 2. Furnace Control Schematic.

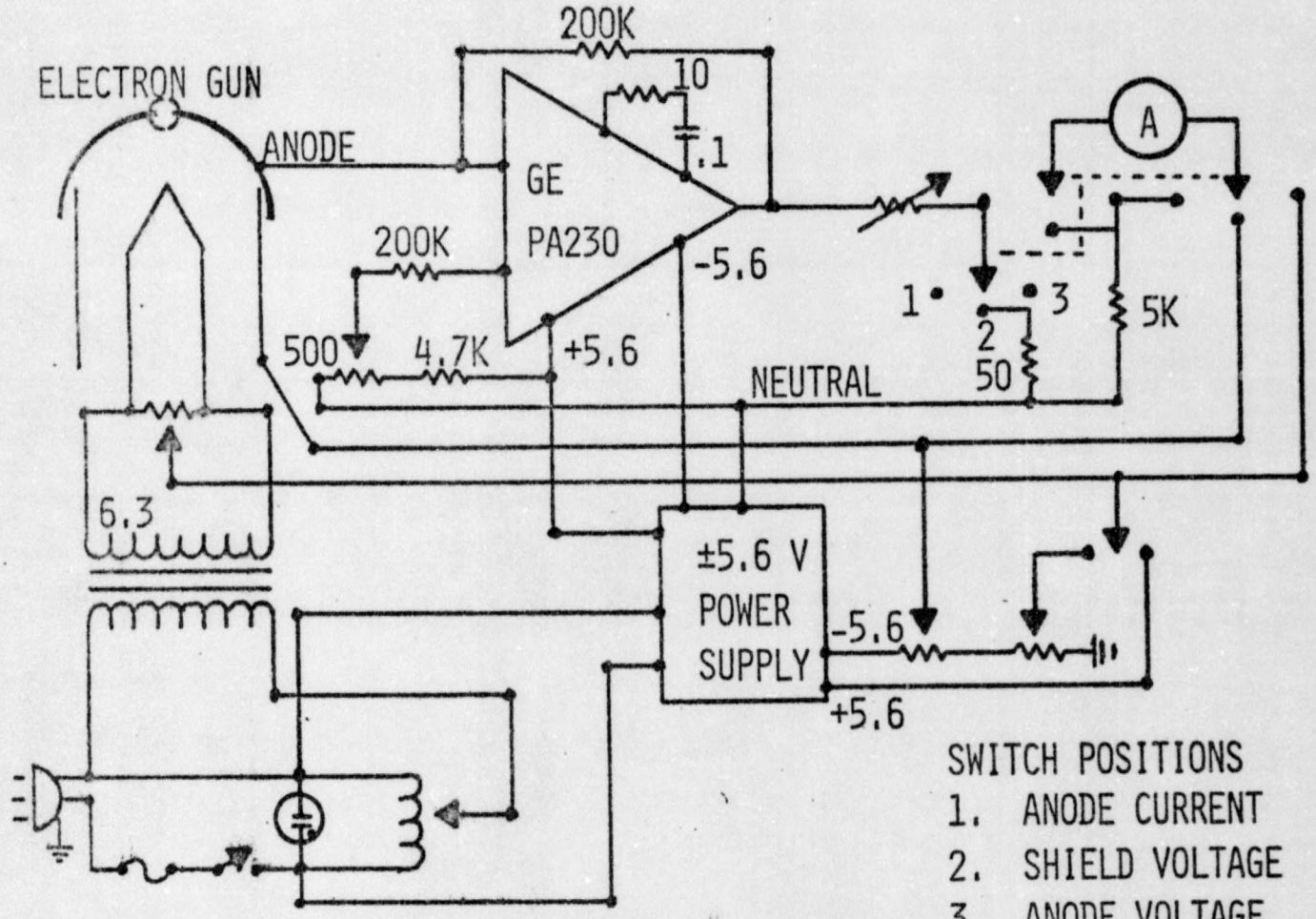

APPENDIX 3. ELECTRON GUN CONTROL.

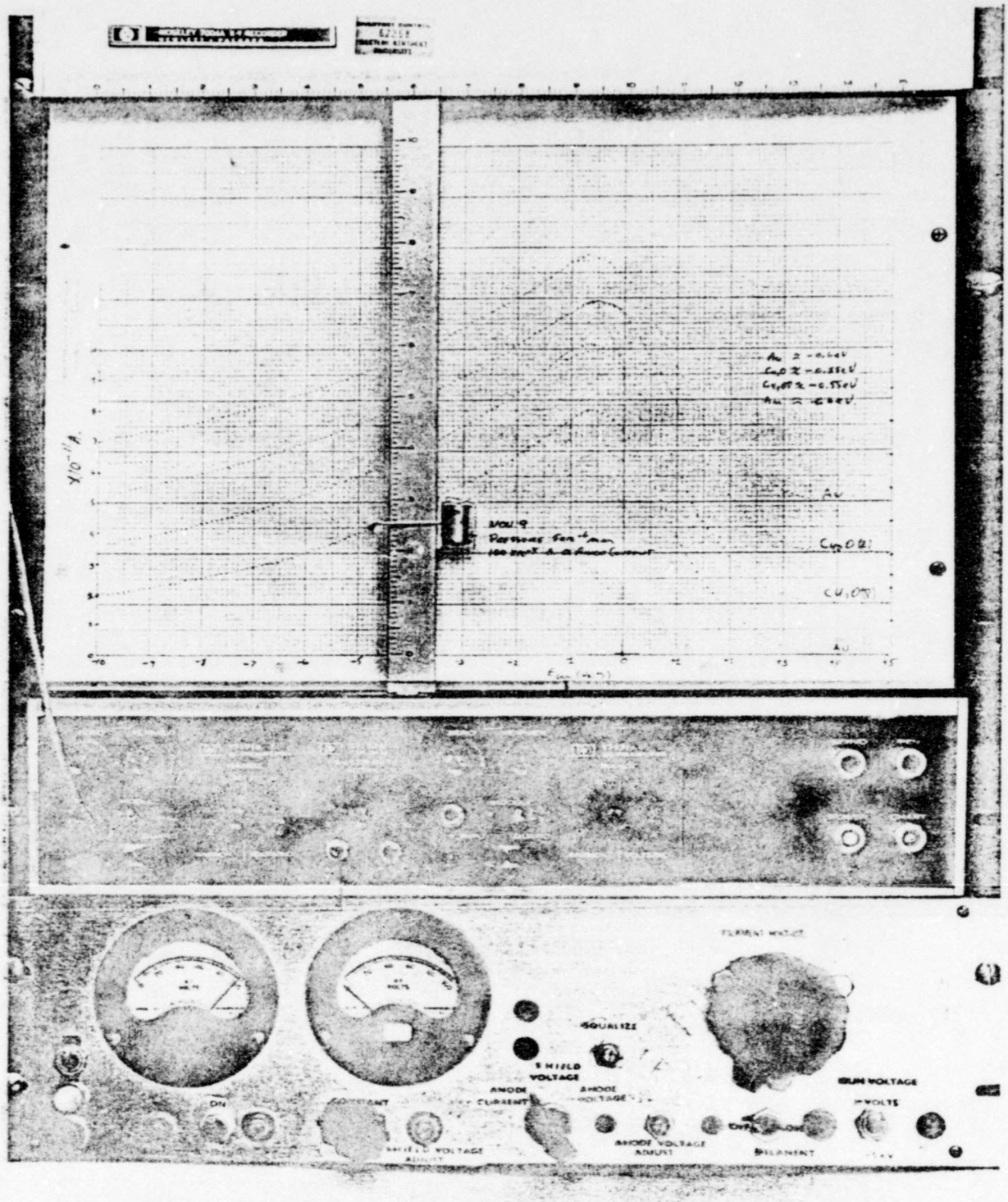

APPENDIX 4. ELECTRON GUN CONTROL PANEL AND X-Y RECORDER.

LIGHT SOURCE WAVELENGTH (Å)	STANDARD MERCURY LINES (Å)	PHOTON ENERGY (eV)
2505	2482	4.993
2560	2536	4.887
2675	2654	4.644
2820	2814	4.426
2910	2893	4.284
2990	2967	4.177
3040	3025	4.1
3150	3131	3.96

STANDARD LINES TAKEN FROM CRC HANDBOOK AND FROM KOMP [8].

APPENDIX 5. LIGHT CALIBRATION.

REFERENCES

1. F. L. Weichman and R. Kuzel, J. Appl. Phys., 41, 3491 (1970).

2. C. Wagner and H. Hammen, Z. Physik. Chem. (Leipzig), B40, 197 (1938).

3. C. A. Hogarth, Z. Physik. Chem. (Leipzig), 198, 30 (1951).

4. M. H. Zirin and D. Trivich, J. Chem. Phys., 39, 870 (1963).

5. M. R. Wright, Hall Effect and Electrical Conductivity of Monocrystalline Cuprous Oxide, Ph. D. Dissertation, Wayne State University, Detroit, Michigan (1962).

6. E. Fortin and F. L. Weichman, Can. J. Phys., 44, 1551 (1966).

7. R. Kuzel and F. L. Weichman, Can. J. Phys., 48, 1585 (1970).
R. Kuzel and F. L. Weichman, J. Appl. Phys., 41, 271 (1970).
R. Kuzel and F. L. Weichman, Can. J. Phys., 48, 63 (1970).

8. R. J. Komp, Photoelectric Emission from Single Crystal Cuprous Oxide, Ph. D Dissertation, Wayne State University, Detroit, Michigan (1964). Detroit Michigan (1964).

9. A. Ioffe, Zhur. Ekspr. Tlev. Fiz., 15, 721 (1945).

10. P. A. Anderson, Phys. Rev., 88, 655 (1952).

11. R. C. Nelson, J. Opt. Soc. Am., 46, 1016 (1956).

12. R. J. Komp and T. J. Fitzsimmons, Photochem. and Photobio., 8, 419 (1968).

13. P. A. Anderson, Phys. Rev., 115, 553 (1959).

14. E. E. Huber, Jr., App. Phys. Letters, 8, 169 (1966).

15. P. A. Anderson, Phys. Rev., 76, 388 (1949).

16. P. A. Anderson, Phys. Rev., 75, 1205 (1949).

17. E. Wigner and J. Bardeen, Phys. Rev., 48, 84 (1935).

18. R. H. Fowler, Phys. Rev., 38, 45 (1931).
L. A. DuBridge, Phys. Rev., 39, 108 (1932).

19. T. E. Fischer, Surface Science, 13, 30 (1969).

20. L. Apker, E. Taft, and J. Dickey, Phys. Rev., 74, 1462 (1948).

21. E. O. Kane, Phys. Rev., 127, 131 (1962).

22. F. G. Allen and G. W. Gobeli, Phys. Rev., 127, 150 (1962).
F. G. Allen and G. W. Gobeli, Phys. Rev., 127, 141 (1962).

23. W. E. Spicer, Phys. Rev., 112, 114 (1958).

24. J. Bloem, Philips Res. Repts., 13, 167 (1958).
cf. G. F. J. Garlick, Photoconductivity, Handbuch der Physik, XIX, 377 (1956).

25. J. P. Dahl and A. C. Switendick, J. Phys. Chem. Solid, 27, 931 (1966).

26. V. P. Smirnov, Soviet Physics - Solid State, 8, 2020 (1962).

27. E. F. Gross, Soviet Physics - Doklady, 5, 531, (1960).

28. A. G. Zhilich and V. P. Makarov, Soviet Physics - Solid State, 3, 429 (1960).

29. V. P. Smirov, Soviet Physics - Solid State, 7, 2312 (1966).

30. S. Brahams and S. Nikitine and J. P. Dahl, Physics Lett., 22, 31 (1961).

31. A. F. Ioffe, Physics Of Semiconductors, (Academic Press Inc., New York, 1960), p. 78.

32. R. Kuzel, Czech. J. Phys., B15, 709 (1965).

33. J. D. Schick and D. Trivich, J. Electrochem. Soc.: Solid-State Sciences and Technology, 119, 376 (1972).

34. R. S. Toth, R. Kilson, and D. Trivich, J. Appl. Phys., 11, 1117 (1960).

35. P. A. Kotsyumakha, Y. A. I. Kushnir, and A. V. Perelygin, Nauk. SSSR, Ser. Fiz., 28, 1328 (1964).

AUTOBIOGRAPHICAL SKETCH

James Ryan Lindle was born in Sturgis, Kentucky on May 31, 1949. After graduating from Union County High School, he enrolled at Western Kentucky University where he received a B.S. degree in Physics and Mathematics in May 1971. He then entered the Graduate School at Western in the fall of 1971, and received a M.S. degree in Physics in August 1973.

Ryan is a member of the Society of Physics Students (SPS), Honorary Physics Society and Western's Honor Program.

As an undergraduate, he worked under the supervision of Dr. Richard Komp. Together they designed and constructed a two-zone vertical furnace and an automatic stereo furnace controller. This system was stable within 3 ^{o}C at 1090 ^{o}C for a period of 24 hrs. After completing the furnace and controller, cuprous oxide monocrystals were grown. These crystals were subjected to electrical conductivity and photoconductivity experiments. These experiments were conducted in air as well as in an evacuated cryogenic apparatus.

Under the supervision of Dr. William Buchman, Ryan conducted experiments to determine the effect of radiation on the learning in the planaria. Before the planaria were irradiated, they were conditioned to respond positively to

a photo-stimuli. The retention of this learned response was studied after irradiation.

In November 1972, Ryan presented a paper on "Electron-Beam Retardation Contact Potential of Cuprous Oxide" at the Southeast Section of the American Physical Society meeting in Birmingham, Alabama.

Ryan also helped setup the Biophysics lab and the Radiological Health lab. He was a lab assistant in Nuclear lab and in Computer lab. As a research tool he wrote substantial computer programs to show proficiency in the following languages: Focal, Fortran IV, PL/I, Basic, and Assembler language.

As a graduate teaching assistant, he taught 101 Physics and the associated lab.